Published for SISSA by Springer
Received: November 22, 2017
Accepted: December 11, 2017
Published: December 18, 2017

Flavor gauge models below the Fermi scale

K.S. Babu,[a] **A. Friedland,**[b,1] **P.A.N. Machado**[c,d,2] **and I. Mocioiu**[e]

[a] *Department of Physics, Oklahoma State University, Stillwater, OK 74078, U.S.A.*
[b] *SLAC National Accelerator Laboratory, Stanford University, Menlo Park, CA, 94025, U.S.A.*
[c] *Departamento de Física Teórica and Instituto de Física Teórica, IFT-UAM/CSIC, Universidad Autónoma de Madrid, Cantoblanco, 28049, Madrid, Spain*
[d] *Theoretical Physics Department, Fermi National Accelerator Laboratory, Batavia, IL, 60510, U.S.A.*
[e] *Department of Physics, The Pennsylvania State University, University Park, PA 16802, U.S.A.*

E-mail: babu@okstate.edu, alexfr@slac.stanford.edu, pmachado@fnal.gov, ium4@psu.edu

Abstract: The mass and weak interaction eigenstates for the quarks of the third generation are very well aligned, an empirical fact for which the Standard Model offers no explanation. We explore the possibility that this alignment is due to an additional gauge symmetry in the third generation. Specifically, we construct and analyze an explicit, renormalizable model with a gauge boson, X, corresponding to the $B-L$ symmetry of the third family. Having a relatively light (in the MeV to multi-GeV range), flavor-nonuniversal gauge boson results in a variety of constraints from different sources. By systematically analyzing 20 different constraints, we identify the most sensitive probes: kaon, B^+, D^+ and Upsilon decays, $D-\bar{D}^0$ mixing, atomic parity violation, and neutrino scattering and oscillations. For the new gauge coupling g_X in the range $(10^{-2}$–$10^{-4})$ the model is shown to be consistent with the data. Possible ways of testing the model in b physics, top and Z decays, direct collider production and neutrino oscillation experiments, where one can observe nonstandard matter effects, are outlined. The choice of leptons to carry the new force is ambiguous, resulting in additional phenomenological implications, such as non-universality in semileptonic bottom decays. The proposed framework provides interesting connections between neutrino oscillations, flavor and collider physics.

Keywords: Beyond Standard Model, Gauge Symmetry, Kaon Physics, Neutrino Physics

ArXiv ePrint: 1705.01822

[1] ORCID: http://orcid.org/0000-0002-5047-4680.
[2] ORCID: http://orcid.org/0000-0002-9118-7354.

https://doi.org/10.1007/JHEP12(2017)096

JHEP12(2017)096

Contents

1 Introduction

One of the long-standing puzzles of the Standard Model (SM) is the origin of flavor: understanding why all fermion fields come in three families, or generations. Within each family the gauge quantum numbers are perfectly coordinated to cancel all 10 potential gauge anomalies (see for e.g., [1]), ensuring the theoretical consistency of the SM as a chiral gauge theory [2]. In contrast, the SM has no similar consistency condition that would

JHEP12(2017)096

require combining particles of *different* generations. In this sense, while every member of a given family is indispensable for making that family consistent, the different families do not seem to have a need for one another.

In searching for answers to the fundamental questions of flavor physics, the first step is to understand the physical properties of the generations. Here again Nature offers a puzzle: in the SM the families are identical copies of each other in some characteristics, but not all. Specifically, partners from different generations are thought to have exactly the same (*universal*) gauge interactions, while their Yukawa couplings to the Higgs field are vastly different, as reflected by their masses. Perhaps the Yukawa and gauge interactions are unrelated? Yet, the pattern of the mixing angles in the CKM matrix does not appear random. This is especially so for the third family quarks, which are the most massive of the six and mix little with the first two generations. Explicitly, the top quark (a mass eigenstate) upon emitting the W gauge boson becomes very nearly the bottom quark mass eigenstate. This accurate alignment of the flavor and mass bases seems like an odd coincidence and suggests some underlying connection between the gauge and Yukawa interactions.

Here, we explore a possibility that this alignment of the eigenstates is a sign that the gauge interactions are actually not strictly universal. The idea is simple: if the third generation is charged under an additional gauge group, it cannot mix with the first two using the SM Higgs field. Notice that this is merely a statement of charge conservation, so that the new gauge coupling need not be large. This implies that once the new gauge group is broken somewhere in the vicinity of the weak scale, as we discuss below, the mediator of the new force can be quite light. This may sound dangerous from flavor violation constraints, but as we will see, there is a well-defined allowed region of the parameter space.

How do we choose the new gauge interaction to assign to the third generation? As our guiding principle, we wish to preserve the elegant feature of the SM outlined above: that all anomalies cancel *within a generation*. It is well known that the simplest gauge group with such properties is based on the difference of the baryon and lepton numbers, $\mathrm{U}(1)_{B-L}$, provided one adds a right-handed sterile neutrino to cancel the cubic anomaly. Thus, *this paper is devoted to the phenomenology of the weakly gauged* $\mathrm{U}(1)^{(3)}_{B-L}$.

Let us briefly review how our framework is different from the existing literature. The observation that $\mathrm{U}(1)_{B-L}$ is anomaly free and can be gauged has been made four decades ago and has been studied in numerous contexts. The classical framework [3–6] considers this symmetry to be flavor-universal and broken at a high scale, so that the lepton-number violating (LNV) Majorana mass for the sterile neutrino is generated and LNV effects are then transmitted to the light neutrinos via the seesaw mechanism. More recently, $B-L$ was considered to be broken at the low scale, but again in a strictly flavor-universal setup [7]. Some additional constraints on this low-scale mediator were obtained in [8]. None of these cases consider flavor-nonuniversality. New light physics is also flavor-universal in another class of models, those involving a dark photon, which interacts with the SM via kinetic mixing [9]. Finally, there have been ideas to study flavor-dependent, horizontal gauge symmetries [10] (for related discussions in a dynamical electroweak symmetry breaking context, see e.g. refs. [11, 12]). Gauging the symmetry based on $L_\mu - L_\tau$ [13] has attracted quite a bit of interest in recent years [14–22]. While such new interactions would be also

JHEP12(2017)096

anomaly-free, the cancellation is achieved between generations. This class of model is very different from ours, both in terms of its philosophy and its physics.

Let us outline some of the generic consequences of gauging $\mathrm{U}(1)^{(3)}_{B-L}$. The most obvious one is the existence of an extended Higgs sector. Indeed, in addition to the Higgs field with the SM quantum numbers (henceforth ϕ_2), a new field, ϕ_1, charged under the new gauge symmetry is required, to allow for nonzero mixing between the third family and the first two. As we will see, to make the theory phenomenologically viable, one also needs to introduce another scalar field, s, that is a singlet under $\mathrm{SU}(3)_c \times \mathrm{SU}(2)_L \times \mathrm{U}(1)_Y$, but is charged under $\mathrm{U}(1)^{(3)}_{B-L}$. Together, the vacuum expectation values of ϕ_1 and s will spontaneously break $\mathrm{U}(1)^{(3)}_{B-L}$, giving a mass M_X to the new gauge boson X. Moreover, the vacuum expectation value (VEV) of ϕ_1 will mix the X with the electroweak Z boson.

Because of the $X - Z$ mixing, the new force will actually couple not only to the third generation, but also to the first two, with appropriate suppression factors. This is the second generic consequence of our framework. The model predicts additional neutral currents and one has to carefully ensure existing tight bounds are not violated. This means analyzing a plethora of constraints and identifying the dominant ones for different values of the mediator mass M_X. Needless to say, we are required to dispense with the effective field theory descriptions that are usually assumed when analyzing new flavor physics constraints (see for example [23]). When the new gauge boson is light, one should of course keep it in the low energy spectrum as a dynamical field, all the way down to energy scales below its mass.

The analysis of the neutral currents also extends to the lepton sector. Here, we find our third general prediction: the neutrinos will interact non-universally with matter and the MSW potential will gain additional terms. Thus, our framework is a model of neutrino non-standard interactions (NSI), which have been of phenomenological interest to the oscillation community for a number of years [24–38]. It is remarkable that in some parts of the parameter space neutrino oscillations already provide important constraints on the model. It is also remarkable that these NSI effects probe a certain combination of the Higgs vacuum expectation values (VEVs) at the weak-scale and not the light mass M_X. Of course, the effects are communicated to our sector via X, but the value of M_X drops out from the oscillation potential.

Another important class of constraints, in which the mass M_X drops out, is made up of processes dominated by the longitudinal mode of X. As seen below, the relevant mode is actually properly understood as the Goldstone from the extended Higgs sector that is eaten by X. As a consequence, the relevant rates depend only on the Yukawa couplings and not on g_X. These bounds therefore apply even in the limit of infinitesimally gauged (global) $\mathrm{U}(1)^{(3)}_{B-L}$.

It should be by now obvious that the analysis of this model is by necessity very rich: we investigate over twenty potential constraints. Of these, we identify a subset of essential bounds: they come from Υ, Kaon and B decays, D decays and $D - \bar{D}$ oscillations, atomic parity violation, neutrino oscillations and electroweak precision observables. Each of these becomes dominant in some parts of the parameter space. Of course, to be sure that the other dozen constraints are subdominant, we are required to evaluate them as well. To

JHEP12(2017)096

keep the scope of the paper finite, we deliberately do not include any discussions of the astrophysical constraints here. We also do not consider in details certain model-building aspects and collider constraints. They will be covered in separate publications.

Before turning to our main presentation, two important comments about the lepton sector of the theory have to be made. First, what we call "the third generation leptons" is strictly speaking *a priori* ambiguous: since there are no gauge bosons connecting the third generation quarks with the lepton sector the same way the top and bottom quarks are connected, we do not know that it is the τ lepton that has to be assigned $\mathrm{U}(1)^{(3)}_{B-L}$. In fact, any linear combination of the leptons from the three generation can be used to cancel the anomalies of the third family quarks and hence any such combination could be made charged under the new gauge group. We stick with τ and ν_τ as the "the third generation leptons" only for definiteness. This choice is made to once again keep the scope of the present paper manageable.

Second, so far we have avoided any mention of the leptonic mixing, which is clearly different from the pattern in the quark sector. This qualitative difference already points to the different physical origin of the neutrino masses compared to those of quarks. Indeed, we will see this when we briefly discuss the framework for neutrino masses below. Our masses are of Majorana type and can be obtained from seesaw-type relations. Notice that one important difference compared to the classical seesaw is that the right-handed $B-L$ partner neutrino (required by anomaly cancellation) lives near the scale of the Higgs VEVs, where the gauge symmetry is broken. Therefore, there are physical arguments to expect the neutrino mass mechanism in our model to be potentially within reach of collider physics.

The rest of the paper is organized as follows. In section 2 we present and analyze the $\mathrm{U}(1)^{(3)}_{B-L}$ model. Section 3 provides a summary of the main experimental constraints on the model. Section 4 discusses other low energy constraints on the model. In section 5 we discuss some important overall consequences of our findings and provide an outlook for future searches for this scenario.

2 The $\mathrm{U}(1)^{(3)}_{B-L}$ model

The model we study is based on the Standard Model symmetry extended by a $\mathrm{U}(1)^{(3)}_{B-L}$ gauge symmetry. $B-L$ symmetry is anomaly free for each generation of fermions, provided that a right-handed neutrino is introduced. Thus the $\mathrm{U}(1)^{(3)}_{B-L}$ charges of fermions in our extended model are $(Q_{3L}, u_{3R}, d_{3R}) : 1/3$, $(\ell_{3L}, e_{3R}, \nu_{3R}) : -1$, with all fermions of the first two families carrying zero charges. This is true for (ν_{1R}, ν_{2R}) as well, and as a result these states could in principle acquire large Majorana masses and decouple from the low energy theory. We do use these states for neutrino mass generation through effective seesaw operators.

The gauge boson associated with $\mathrm{U}(1)^{(3)}_{B-L}$ is denoted X, and we shall be interested in the case where M_X is in the MeV-multi-GeV range. Flavor effects have been widely studied when M_X is larger than the electroweak scale, while below about 100 keV stellar cooling bounds typically require the gauge coupling to be so small that such an X boson would be of little interest for flavor phenomenology. Although the mass of X is in the

JHEP12(2017)096

	ϕ_1	ϕ_2	s
$\mathrm{SU}(2)_L$	**2**	**2**	**1**
$\mathrm{U}(1)_Y$	$+1$	$+1$	0
$\mathrm{U}(1)^{(3)}_{B-L}$	$+1/3$	0	$+1/3$

Table 1. Scalar fields and their charges under the Standard Model gauge group and the $\mathrm{U}(1)^{(3)}_{B-L}$ gauge symmetry. In our notation, the $\mathrm{U}(1)^{(3)}_{B-L}$ charge of the third family quarks is $+1/3$, while that for the third family leptons is -1. The first two families of fermions have zero $\mathrm{U}(1)^{(3)}_{B-L}$ charges.

MeV-multi-GeV range, the scale of $\mathrm{U}(1)^{(3)}_{B-L}$ symmetry breaking could be several hundred GeV, which is what we shall take as our benchmark value. This is possible owing to the smallness of the gauge coupling g_X.

A minimal scalar sector for the model consists of two Higgs doublets, ϕ_2 with zero $\mathrm{U}(1)^{(3)}_{B-L}$ charge and ϕ_1 carrying U(1) charge of 1/3, as well as a SM singlet field s. The $\mathrm{U}(1)^{(3)}_{B-L}$ charges of the scalars are listed in table 1. ϕ_2 is the Higgs doublet that generates diagonal mass terms for the quarks and leptons, while ϕ_1 induces off-diagonal quark mixing terms involving the third family. The field s is needed for consistent phenomenology as well as for inducing neutrino mixings via simple effective operators. As we shall see, without the singlet field, the contributions to non-standard neutrino oscillations from the X gauge boson will exclude the model. The $\mathrm{U}(1)^{(3)}_{B-L}$ charge of s field is uniquely fixed to be 1/3 or 1/6, other choices would lead to an enhanced global U(1) symmetry in the Higgs potential, resulting in an unwanted pseudo-Goldstone boson. (A term of the type $\phi_1^\dagger \phi_2 s$ or $\phi_1^\dagger \phi_2 s^2$ would break such a global symmetry explicitly and give mass to the Goldstone boson.) We shall focus on s charge being 1/3, which leads to a slightly simpler neutrino mass generation scheme.

Since the Higgs doublet ϕ_1 carries both $\mathrm{U}(1)_Y$ and $\mathrm{U}(1)^{(3)}_{B-L}$ charges, when its neutral component acquires a vacuum expectation value it will induce mixing between the Z and the new gauge boson X. As the new symmetry is an Abelian U(1), the model also admits the possibility of kinetic mixing between the hypercharge gauge boson and the X boson [9].

2.1 The Yukawa sector

Since the third family quarks carry a nonzero $\mathrm{U}(1)^{(3)}_{B-L}$ charge while the first two families do not, the Yukawa couplings that would induce three family quark mixing should involve both doublets ϕ_1 and ϕ_2. The ϕ_1 field is introduced for the purpose of inducing quark mixing with the third family. The Yukawa Lagrangian for the quarks is given by

$$\mathcal{L}^q_{\rm yuk} = \overline{\mathbf{Q}}_L \begin{pmatrix} y^u_{11}\widetilde{\phi}_2 & y^u_{12}\widetilde{\phi}_2 & y^u_{13}\widetilde{\phi}_1 \\ y^u_{21}\widetilde{\phi}_2 & y^u_{22}\widetilde{\phi}_2 & y^u_{23}\widetilde{\phi}_1 \\ 0 & 0 & y^u_{33}\widetilde{\phi}_2 \end{pmatrix} \mathbf{u}_R + \overline{\mathbf{Q}}_L \begin{pmatrix} y^d_{11}\phi_2 & y^d_{12}\phi_2 & 0 \\ y^d_{21}\phi_2 & y^d_{22}\phi_2 & 0 \\ y^d_{31}\phi_1 & y^d_{32}\phi_1 & y^d_{33}\phi_2 \end{pmatrix} \mathbf{d}_R + \text{h.c.} \qquad (2.1)$$

Here the bold symbols stand for vectors in generation space, and $\widetilde{\phi}_i \equiv i\sigma_2\phi_i^*$ with σ_2 being the second Pauli matrix. The simultaneous presence of ϕ_1 and ϕ_2 in the Yukawa couplings

JHEP12(2017)096

of the up-quarks (and similarly for the down-quarks) would imply that there are Higgs-mediated FCNC processes in the model. We shall see that these processes are within acceptable limits, provided that the neutral Higgs bosons have masses of order hundred GeV.

As only the third family carries the new $\mathrm{U}(1)^{(3)}_{B-L}$ charge, the Cabibbo angle can be generated without inducing any FCNC mediated by neutral scalar bosons or the X gauge boson. We thus make 1-2 rotations in both the up- and down- quark sectors, thereby inducing a nonzero $(1,2)$ entry in the CKM matrix. The other CKM matrix elements V_{ub} and V_{cb} can be generated from the rotated mass matrices which can be written in the form

$$R^{uL}_{12}.M_u.R^{uR\dagger}_{12} = \begin{pmatrix} m^0_u & 0 & V^0_{ub}m^0_t \\ 0 & m^0_c & V^0_{cb}m^0_t \\ 0 & 0 & m^0_t \end{pmatrix} \quad \text{and} \quad R^{dL}_{12}.M_d.R^{dR\dagger}_{12} = \begin{pmatrix} m^0_d & 0 & 0 \\ 0 & m^0_s & 0 \\ am^0_b & bm^0_b & m^0_b \end{pmatrix} \tag{2.2}$$

where R_{ij} parametrizes an $i-j$ rotation in terms of a mixing angle and a phase. While these forms are quite general, we shall approximate m^0_i in eq. (2.2) to be nearly equal to the physical eigenvalue m_i and V^0_{ij} to be nearly equal to the actual CKM mixing element V_{ij}.

The down quark mass matrix given in eq. (2.2) is diagonalized by right-handed rotations alone, with the left-handed mixing matrix being very close to an identity matrix. Thus V_{cb} and V_{ub} should arise primarily from the up-quark sector. The FCNC constraints arising from the down-quark sector are more severe compared to those arising from the up-quark sector. Assuming that $m^0_b \simeq m_b$, $B_d - \bar{B}_d$ mixing mediated by the neutral scalar bosons sets a limit $a \lesssim 3\times 10^{-3}/\tan\beta$ for scalar masses of order 100 GeV, while $B_s - \bar{B}_s$ mixing constrains $b \lesssim 10^{-2}/\tan\beta$ on the parameters a and b appearing in the down quark mass matrix in eq. (2.2) (see section 4 for details). Here we have defined $\tan\beta \equiv v_2/v_1$. Similar constraints are obtained from the decays $B_d \to X\gamma \to e^+e^-\gamma$ [39] and $B_s \to X \to \mu^+\mu^-$. More importantly, off-diagonal couplings Xdb and Xsb would contribute to the total width of B_d and B_s, as well as to $B^+ \to \pi^+e^+e^-$ and $B^+ \to \pi^+\mu^+\mu^-$. The first and second widths would constrain $g_X(b/V_{cb}) < 2.8\times 10^{-6}(M_X/100\,\mathrm{MeV})$ and $g_X(a/V_{ub}) < 2.9\times 10^{-5}(M_X/100\,\mathrm{MeV})$, while the last processes would lead to

$$g_X\frac{a}{V_{ub}} < 1.8\times 10^{-10}\frac{M_X/100\,\mathrm{MeV}}{\sqrt{\mathrm{BR}(X\to e^+e^-)}}, \quad g_X\frac{a}{V_{ub}} < 3.8\times 10^{-10}\frac{M_X/100\,\mathrm{MeV}}{\sqrt{\mathrm{BR}(X\to \mu^+\mu^-)}}, \tag{2.3}$$

see appendix A for details.

With these constraints, the parameters a and b in eq. (2.2) cannot significantly contribute to the generation of CKM mixing angles V_{cb} and V_{ub}, which we shall thus ignore. Notice that FCNCs will be induced in the down sector at loop level, and that is particularly important for Kaon decays, as we will see in section 3. Within these assumptions, the left-handed rotations that diagonalize M_u and M_d are given by (in a basis where the 1-2 up-sector is already diagonal, i.e., with R^{uL}_{12}, R^{uR}_{12} being identity matrices)

$$V^L_u = R^{uL}_{23}(V_{cb})R^{uL}_{13}(V_{ub}), \tag{2.4}$$

$$V^{L\dagger}_d = R^{dL}_{12}(V_{us})^\dagger. \tag{2.5}$$

If the X charge of the scalars are instead chosen to be $-1/3$, the Yukawa Lagrangian for up-type quarks and down-type quarks (2.1) would be interchanged. That would suggest

JHEP12(2017)096

the generation of V_{ub} and V_{cb} in the down sector, which would lead to strong constraints in g_X, as discussed above. We do not pursue such possibility in this manuscript. The quark mixing matrix is given by $V_{\rm CKM} = V_u^L V_d^{L\dagger}$. It can be readily checked that a CP violating phase of the correct magnitude is obtained from complex entries of the mass matrices. It follows from eq. (2.2) that any FCNC effects induced by scalar boson exchanges would be weighted by V_{ub} and V_{cb} in the top sector where the experimental constraints are meager, and by $V_{ub}V_{cb}$ in the $u-c$ sector. This suppression factor will be sufficient to avoid the stringent $D^0 - \overline{D^0}$ mixing bounds and mitigate the effect on D^+ decays with $\Delta C = 1$, as we will see in section 3.

In the charged lepton sector Yukawa couplings between the third and the first two families are strictly forbidden owing to the charge assignment and minimality of the Higgs sector of the model. Charged lepton masses arise through the Yukawa Lagrangian involving the ϕ_2 scalar only and is given by

$$\mathcal{L}^{\ell}_{\rm yuk} = y^{\ell}_{ij}\overline{L}_i\phi_2\ell_{Rj}, \tag{2.6}$$

with $y_{ij} = 0$ for $ij = 13, 23, 31, 32$. We see that the leptonic mixing angle θ^{ℓ}_{12} could be generated from here, but not θ^{ℓ}_{23} and θ^{ℓ}_{13}. There are no FCNC processes mediated by the Higgs bosons, since the Yukawa coupling matrix is proportional to the charged lepton mass matrix. There are also no FCNC processes mediated by the X gauge boson, since the mass eigenbasis and the flavor eigenbasis coincide for the charged leptons. The complete absence of tree-level FCNC in the charged lepton sector is a compelling feature of the model, protecting it from the severe bounds that could have arisen from flavor changing muon and tau decays.

Neutrino mass generation calls for additional physics which can however reside at a higher scale. In the minimal setup considered here, we can infer neutrino masses as arising from effective operators via a generalized seesaw mechanism. For the 1-2 sector of the effective Majorana matrix of the light neutrinos, the usual dimension-5 operator can be built (with $\tilde{L}_i \equiv i\tau_2 L_i^*$):

$$\frac{1}{\Lambda}\left(\bar{L}_{1,2}\tilde{\phi}_2\right)\left(\phi_2^{\dagger}\tilde{L}_{1,2}\right), \tag{2.7}$$

while the mixing responsible for θ^{ℓ}_{13} and θ^{ℓ}_{23} should come from a dimension-6 operator

$$\frac{1}{\Lambda^2}\left(\bar{L}_3\tilde{\phi}_1\right)\left(\phi_1^{\dagger}\tilde{L}_{1,2}\right)s^*. \tag{2.8}$$

These operators could be generated by exchanging singlet neutrinos with $\mathrm{U}(1)^{(3)}_{B-L}$ charges 0, $\pm 1/3$ and $\pm 2/3$. The first of those can be identified as the usual right-handed neutrinos of the first two families, while the remaining two are singlet fermions which are vector-like under $\mathrm{U}(1)^{(3)}_{B-L}$. Note that the right-handed neutrino ν_{3R} with $\mathrm{U}(1)^{(3)}_{B-L}$ charge -1 will mix with the vector-like component with charge $\pm 2/3$ via the Yukawa coupling $\nu_{3R}n_{2/3}s$ once the s field acquires a VEV. Thus there are no light sterile neutrinos in the model, provided that the vector-like singlet neutrinos are not too heavy (otherwise the mass of ν_{3R} will become small via a seesaw suppression factor).

JHEP12(2017)096

Since all neutrino mixing angles are relatively large, the mass matrix elements coming from the dimension-5 and the dimension-6 operators should be comparable. If the singlet neutrinos that are integrated out have masses not far above the TeV scale, so that they also do not introduce an additional hierarchy problem for the Higgs boson mass [40], then these different contributions to light neutrino masses would be of the same order. Besides, as ν_{3R} is needed to cancel anomalies, its mass cannot be decoupled from the theory: the mass of this state should be close to or below v_s. As we will see later, typical values for v_s lie between 100–1000 GeV, assuming no new hierarchy problem in the scalar sector is introduced in the model. This provides a deeper reason for why at least part of the sterile neutrino spectrum should be accessible at the LHC. The LHC phenomenology of the neutrino mass generation sector may be pursued in a future manuscript.

2.2 The gauge boson sector

Now we turn our attention to the gauge boson sector. We adopt the convention $q = I_3 + Y/2$ for the hypercharge, where q is the electric charge, $I_3 = 0, \pm 1/2$ for $\mathrm{SU}(2)_L$ singlet and doublet fields, and Y is the hypercharge. The gauge kinetic terms for the scalar fields are given by $\sum_i |D_\mu \phi_i|^2 + |D_\mu s|^2$ where the covariant derivatives are defined as

$$D_\mu \phi_i = \left(\partial_\mu - ig\frac{\tau_i}{2}W_\mu^i - ig'\frac{Y}{2}B_\mu - ig_X q_X X_\mu^0\right)\phi_i, \quad D_\mu s = \partial_\mu s - ig_X q_X s. \tag{2.9}$$

When the scalar fields acquire VEVs, $\mathrm{SU}(2)_L \times \mathrm{U}(1)_Y \times \mathrm{U}(1)_{B-L}^{(3)}$ symmetry breaks spontaneously down to $\mathrm{U}(1)_{em}$. Since the doublet field ϕ_1 is charged under both Y and $\mathrm{U}(1)_{B-L}^{(3)}$, its VEV will induce mixing between the Z and the new gauge boson X. In the absence of kinetic mixing the gauge boson mass-squared matrix is given as (in the basis (Z^0, X^0) where the 0 subscript indicates a state before $Z - X$ mixing)

$$M_{\text{gauge}}^2 = \frac{1}{4}\begin{pmatrix} (g^2+g'^2)v^2 & -2\sqrt{g^2+g'^2}g_X v_1^2/3 \\ -2\sqrt{g^2+g'^2}g_X v_1^2/3 & 4g_X^2(v_1^2+v_s^2)/9 \end{pmatrix}. \tag{2.10}$$

Here v_1, v_2, v_s are the VEVs of ϕ_1, ϕ_2, and s, respectively, with $v_1^2 + v_2^2 \equiv v^2 = (246\,\text{GeV})^2$. The photon is still the combination $A_\mu = c_w B_\mu + s_w W_\mu^3$ ($c_w = \cos\theta_w$, $s_w = \sin\theta_w$, $\tan\theta_w = g'/g$), while the physical Z and X boson eigenstates are given by (ignoring terms of order $\mathcal{O}(g_X^2)$),

$$Z_\mu \simeq -s_w B_\mu + c_w W_\mu^3 - s_X X_\mu^0, \tag{2.11}$$

$$X_\mu \simeq s_X(-s_w B_\mu + c_w W_\mu^3) + X_\mu^0, \tag{2.12}$$

with the $Z - X$ mixing angle s_X defined as

$$s_X \equiv \frac{2}{3}\frac{g_X}{\sqrt{g^2+g'^2}}\frac{v_1^2}{v^2}. \tag{2.13}$$

We observe that it is the VEV of ϕ_1 that induces the $Z - X$ mixing, and that s_X is proportional to g_X and v_1. The mass of the X gauge boson is obtained as

$$M_X^2 = \frac{1}{9}g_X^2\left(\frac{v_1^2 v_2^2}{v^2} + v_s^2\right). \tag{2.14}$$

JHEP12(2017)096

Notice that a nonzero v_s can only raise M_X. When v_1 and v_2 are comparable, M_X is essentially fixed in terms of v_s, while for large $\tan\beta$ there is some dependence on v_1 and v_2 as well. Then, for a given g_X, eq. (2.14) defines a minimum mass for the X boson.

As will be seen later, the longitudinal mode X_L plays a prominent role on the phenomenology, particularly in the case of light X (with respect to the scale of the process in question). In such case, the equivalence theorem implies that X_L can be substituted by its corresponding Goldstone boson G_X. It is easy to see that G_X is given by

$$G_X = \frac{1}{3}\frac{g_X}{M_X v^2}\left[-v_1 v_2^2\,\mathrm{Im}(\phi_1^0) + v_1^2 v_2\,\mathrm{Im}(\phi_2^0) - v^2 v_s\,\mathrm{Im}(s^0)\right]. \tag{2.15}$$

Some of the Goldstone boson couplings will be particularly important, namely,

$$\begin{aligned}\mathcal{L}_{G_X} = {} & iG_X\frac{g_X}{3}\frac{m_t}{M_X}\left[-\frac{v_1^2}{v^2}\bar{t}\gamma_5 t + V_{cb}(\bar{c}_L t_R - \bar{t}_R c_L) + V_{ub}V_{cb}(\bar{c}_L u_R - \bar{u}_R c_L)\right] \\ & - iG_X\frac{g_X}{3}\frac{m_\tau}{M_X}\frac{v_1^2}{v^2}\bar{\tau}\gamma_5\tau + \ldots\end{aligned} \tag{2.16}$$

We shall use these couplings when deriving the constraints from decays of various particles into longitudinal modes of X boson.

The gauge boson kinetic terms allow for mixing between $X_{\mu\nu}$ and $B_{\mu\nu}$ parametrized by ε. These are given by

$$\mathcal{L}_{\rm kin} = -\frac{1}{4}W^3_{\mu\nu}W^{3\mu\nu} - \frac{1}{4}B_{\mu\nu}B^{\mu\nu} - \frac{1}{4}X_{\mu\nu}X^{\mu\nu} + \frac{\varepsilon}{2}X_{\mu\nu}B^{\mu\nu} \tag{2.17}$$

$$= -\frac{1}{4}A_{\mu\nu}A^{\mu\nu} - \frac{1}{4}Z_{\mu\nu}Z^{\mu\nu} - \frac{1}{4}X_{\mu\nu}X^{\mu\nu} + \frac{\varepsilon}{2}X_{\mu\nu}(c_w A^{\mu\nu} - s_w Z^{\mu\nu}) + \mathcal{O}(\varepsilon^3). \tag{2.18}$$

To obtain canonical kinetic terms for the gauge bosons, up to $\mathcal{O}(\varepsilon^3)$, the photon and the X fields can be redefined as [41]

$$A_\mu \to A_\mu + \varepsilon c_w X_\mu, \tag{2.19}$$

$$X_\mu \to X_\mu - \varepsilon s_w Z_\mu. \tag{2.20}$$

The effect of the photon field shift is only to couple the standard electromagnetic current to X, with the coupling strength being εc_w. The X field shift has two effects. First, it couples the X current to the Z charge, so the Z couplings to particles that are charged under the new symmetry are slightly modified. Second, as X is massive, its shift gives rise to a $Z - X$ mass term $-2\varepsilon s_w M_X^2$. Assuming $M_X \ll M_Z$, a small rotation by $\varepsilon M_X^2/M_Z^2$ is required to have diagonal mass terms for the Z and X bosons. Due to the additional suppression factor M_X^2/M_Z^2, this rotation is not significant, and we shall neglect this effect. It is important to notice that the non-unitary character of the shift assures the absence of millicharged particles: although electrically charged particles acquire small X charges, the opposite, viz., particles charged under X acquiring small electric charge, does not happen.

Since the $\mathrm{U}(1)^{(3)}_{B-L}$ gauge interaction distinguishes flavor, it leads to FCNCs. In the flavor basis the X interactions to SM fermions are given by

$$\mathcal{L}_{ffX} = c_\alpha \bar{f}_\alpha \gamma_\mu f_\alpha X^\mu, \quad \text{with} \quad c_\alpha = q_\alpha c_w e\,\varepsilon + \left(g_X q_\alpha^X + s_X\sqrt{g^2+g'^2}\,q_\alpha^Z\right), \tag{2.21}$$

JHEP12(2017)096

where q_α, q_α^X, and $q_\alpha^Z = I_3^\alpha - s_w^2 q_\alpha$, are the electric charge, the X charge and the Z charge, respectively, of the fermion α. Notice that, as c_α depends on the chirality of the field, it is not possible to have an accidental cancellation between ε and g_X for both L and R components of any particle. The relative sign (and magnitude) between ε and g_X is physically observable.

We can understand the FCNC processes induced by the X gauge boson by writing the non-universal piece of the interaction explicitly as

$$\mathcal{L}_{\text{X-FCNC}} = \frac{g_X}{3}\overline{\mathbf{Q}}_L \begin{pmatrix} 0 & 0 & 0 \\ 0 & 0 & 0 \\ 0 & 0 & 1 \end{pmatrix} \gamma^\mu \mathbf{Q}_L X_\mu, \tag{2.22}$$

which becomes, after rotating the quarks to the physical basis,

$$\mathcal{L}_{\text{X-FCNC}} \simeq \frac{g_X}{3}\overline{\mathbf{u}}_L \begin{pmatrix} V_{ub}^2 & V_{ub}V_{cb} & V_{ub} \\ V_{ub}V_{cb} & V_{cb}^2 & V_{cb} \\ V_{ub} & V_{cb} & 1 \end{pmatrix} \gamma^\mu \mathbf{u}_L X_\mu + \frac{g_X}{3}\overline{\mathbf{d}}_L \begin{pmatrix} 0 & 0 & 0 \\ 0 & 0 & 0 \\ 0 & 0 & 1 \end{pmatrix} \gamma^\mu \mathbf{d}_L X_\mu. \tag{2.23}$$

The FCNC in the up sector induces flavor-changing top quark decays $t \to uX, cX$ which is presently not much constrained, and it contributes to $D^0 - \bar{D}^0$ mixing and D^+ decays. Note that the $D^0 - \bar{D}^0$ mixing is doubly suppressed by the $V_{ub}V_{cb}$ factor and by the smallness of g_X. We emphasize that there are no FCNC mediated by the X gauge boson in the charged lepton sector, since the corresponding mass matrix is diagonal.

2.3 The scalar potential

Now we turn our attention to the scalar sector of the model. The most general renormalizable scalar potential involving ϕ_1, ϕ_2 and s that respects the symmetry of the model is given by

$$\begin{aligned} V = {} & m_{11}^2(\phi_1^\dagger\phi_1) + m_{22}^2(\phi_2^\dagger\phi_2) + m_s^2 s^* s + \frac{\lambda_1}{2}(\phi_1^\dagger\phi_1)^2 + \frac{\lambda_2}{2}(\phi_2^\dagger\phi_2)^2 + \lambda_3(\phi_1^\dagger\phi_1)(\phi_2^\dagger\phi_2) \\ & + \lambda_4(\phi_1^\dagger\phi_2)(\phi_2^\dagger\phi_1) + \frac{\lambda_s}{2}(s^*s)^2 + \lambda_{1s}(\phi_1^\dagger\phi_1)(s^*s) + \lambda_{2s}(\phi_2^\dagger\phi_2)(s^*s) - \Big[\mu(\phi_2^\dagger\phi_1)s + \text{h.c.}\Big]. \end{aligned} \tag{2.24}$$

The presence of the s field which allows for the cubic scalar coupling μ has several important consequences. First, it removes an unwanted global symmetry and the associated pseudo-Goldstone boson that would exist in its absence. (The charge of the s field is chosen precisely to achieve this.) Second, the μ term allows to take the *decoupling limit* of the model: by making $\mu \to \infty$, $v_s \to \infty$ and $m_{11} \to \infty$ (in order to keep v_1 finite), all extra scalars, the extra gauge boson, and the right-handed neutrinos can be made arbitrarily heavy, so that the low energy theory is the SM. Without this term, the masses of the second Higgs doublet would have been bounded by about 600 GeV, analogous to the two Higgs doublet models with a spontaneously broken discrete Z_2 symmetry [42]. This decoupling behavior of s enabled by μ is essential to evade large deviations in Υ and D^+ decays, atomic parity violation and neutrino experiments.

JHEP12(2017)096

The physical scalar spectrum consists of three neutral scalars, one of which should be identified with the 125 GeV SM-like Higgs, a pseudoscalar, and a charged scalar. A pair of pseudoscalars and a charged scalar are absorbed by the Z, X and $W^{\pm}$ gauge bosons. The physical pseudoscalar boson mass is given by

$$m_A^2 = \mu \frac{v_1^2 v_2^2 + v_1^2 v_s^2 + v_2^2 v_s^2}{\sqrt{2} v_1 v_2 v_s}. \tag{2.25}$$

The charged scalar has a mass given by

$$m_{H^{\pm}}^2 = \frac{1}{2}\lambda_4 v^2 + \mu \frac{v_s v^2}{\sqrt{2} v_1 v_2}, \tag{2.26}$$

while the real scalar mass matrix is given by (in the basis $(\mathrm{Re}(\phi_1), \mathrm{Re}(\phi_2), \mathrm{Re}(s))$

$$m_H^2 = \begin{pmatrix} \lambda_1 v_1^2 + \mu \frac{v_2 v_s}{\sqrt{2} v_1} & (\lambda_3 + \lambda_4) v_1 v_2 - \frac{\mu v_s}{\sqrt{2}} & \lambda_{1s} v_1 v_s - \mu \frac{v_2}{\sqrt{2}} \\ (\lambda_3 + \lambda_4) v_1 v_2 - \frac{\mu v_s}{\sqrt{2}} & \lambda_2 v_2^2 + \mu \frac{v_1 v_s}{\sqrt{2} v_2} & \lambda_{2s} v_2 v_s - \mu \frac{v_1}{\sqrt{2}} \\ \lambda_{1s} v_1 v_s - \mu \frac{v_2}{\sqrt{2}} & \lambda_{2s} v_2 v_s - \mu \frac{v_1}{\sqrt{2}} & \lambda_s v_s^2 + \frac{\mu v_1 v_2}{\sqrt{2} v_s} \end{pmatrix}. \tag{2.27}$$

Although it is not easy to write down simple analytic expressions for the masses and mixings of the real scalars as functions of the parameters of the potential, we still can understand the interplay between the mixing in the scalar sector and the symmetry structure of the model by very simple arguments. ϕ_2 has diagonal couplings to quarks and leptons which cannot distinguish between the $\mathrm{Re}(\phi_1)$ and $\mathrm{Re}(s)$ components of the physical SM-like Higgs, h. These couplings to fermions have the structure $m_f/v_2\, \phi_2 \bar{f} f$, and since $v_1^2 + v_2^2 = v^2$, with $v \simeq 246\,\mathrm{GeV}$, the Yukawa couplings are always larger compared to the SM Yukawas. For the top-quark Yukawa coupling to be in the perturbative range, v_2 cannot be much smaller than v. The scalar ϕ_1 couples off-diagonally to quarks (mediating flavor changing processes). In order to have perturbative Yukawa couplings with the top, $\tan\beta$ should lie in the range between 0.5 and 30, with the upper limit arising from the off-diagonal Yukawa coupling equal to $V_{cb} m_t / v_1$.

To understand the SM-like Higgs FCNC couplings, it is better to go to the Higgs basis, in which $H = c_\beta \phi_1 + s_\beta \phi_2$ and $H' = -s_\beta \phi_1 + c_\beta \phi_2$, which leads to $\langle H \rangle = v$, and $\langle H' \rangle = 0$. Here, $H = (H^+, (h+v)/\sqrt{2})$. The mass matrix in the basis $(\mathrm{Re}(H), \mathrm{Re}(H'), \mathrm{Re}(s))$, to leading order in each entry assuming $v \ll \mu, v_s$ is given by

$$\mathcal{M}^2 \simeq \begin{pmatrix} \frac{\left[\left(\lambda_2 t_\beta^2 + 2\lambda_{34}\right) t_\beta^2 + \lambda_1\right] v^2}{\left(t_\beta^2+1\right)^2} & \frac{t_\beta \left[(\lambda_{34} - \lambda_2) t_\beta^2 + \lambda_1 - \lambda_{34}\right] v^2}{\left(t_\beta^2+1\right)^2} & \frac{\left[\left(\lambda_{2s} t_\beta^2 + \lambda_{1s}\right) v_s - \sqrt{2} t_\beta \mu\right] v}{t_\beta^2 + 1} \\ & \frac{\left(t_\beta^2+1\right) \mu v_s}{\sqrt{2} t_\beta} & \frac{\left[2(\lambda_{1s} - \lambda_{2s}) t_\beta v_s + \sqrt{2}(1 - t_\beta^2)\mu\right] v}{2\left(t_\beta^2+1\right)} \\ & & \lambda_s v_s^2 \end{pmatrix}, \tag{2.28}$$

where we have defined $\lambda_{34} = \lambda_3 + \lambda_4$. The first entry is the SM-like Higgs state, the second is the flavor changing Higgs and the third refers to the state which does not couple to fermions. Integrating out the heavy scalars, when their masses are non-degenerate, yields the effective flavor changing operators

$$y'^u_{ij} \frac{H^\dagger H}{\Lambda^2} \bar{Q}_{iL} \tilde{H} u_{jR} + y'^d_{ij} \frac{H^\dagger H}{\Lambda^2} \bar{Q}_{iL} H d_{jR}, \tag{2.29}$$

JHEP12(2017)096

with

$$y'^{u,d} = y_t \begin{pmatrix} c_\beta m_u/m_t & 0 & -s_\beta V_{ub} \\ 0 & c_\beta m_c/m_t & -s_\beta V_{cb} \\ 0 & 0 & c_\beta \end{pmatrix}, \tag{2.30}$$

a similar matrix for y'^d_{ij}, and also

$$\frac{1}{\Lambda^2} = \frac{1}{(t_\beta^2+1)^2 v_s^2} \left(\frac{t_\beta \left(\lambda_{2,s}-\lambda_{1,s}\right)\left(\lambda_{1,s}+t_\beta^2\lambda_{2,s}\right)}{\lambda_s^2} + \frac{\mu^2\left(t_\beta - t_\beta^3\right)}{\lambda_s^2 v_s^2} \right.$$
$$\left. + \frac{\mu\left(\left(t_\beta^2-3\right)t_\beta^2\lambda_{2,s}+\left(3t_\beta^2-1\right)\lambda_{1,s}\right)}{\sqrt{2}\lambda_s^2 v_s} + \frac{\sqrt{2}v_s t_\beta^2\left(\lambda_1-\lambda_{34}+(\lambda_{34}-\lambda_2)\,t_\beta^2\right)}{\mu\left(t_\beta^2+1\right)} \right). \tag{2.31}$$

This will induce top to charm Higgs decays, which will be analyzed in section 3.

In this basis, the electroweak gauge bosons couple only to H, and hence any mixing of this state can only reduce the couplings of the SM-like Higgs to WW and ZZ. The requirement that the SM-like Higgs boson couples to the gauge bosons with strengths very close to the SM values constrains the admixture of $\mathrm{Re}(H^0)$ with the other scalars. LHC Higgs data constrain the sum of the square of these mixings to be about 0.1 [43]. LHC searches for a heavy Higgs boson decaying to ZZ [44, 45] are sensitive to masses roughly between 200 GeV and 900 GeV, assuming production via gluon fusion and a branching ratio to ZZ similar to a SM-like Higgs of corresponding mass. Due to the structure of the Yukawa couplings the heavy Higgs bosons of the model have suppressed couplings to tt, leading to smaller production cross sections, thus evading the LHC search limits. (Note that in the large $\tan\beta$ limit, $h_{125\mathrm{GeV}} \sim \mathrm{Re}(H^0) \sim \mathrm{Re}(\phi_2^0)$, and since only ϕ_2 has a tt coupling, the couplings of all heavy Higgs bosons with tt will be suppressed by small mixing angles.) Besides, due to the $X - Z$ mixing, the real component of H_1 will couple to X like

$$\mathcal{L}_{hXX} = \frac{g_X^2}{9}\frac{v_1^2 v_2^2}{v^3}\mathrm{Re}(H^0) X_\mu X^\mu. \tag{2.32}$$

This coupling will contribute mainly to the invisible width of the Higgs, as we will see in the next section.

With the aid of the cubic scalar coupling μ the mass of the charged scalar can be raised above the electroweak scale, which may be very important for the following reason. In type-II 2HDM, where each Higgs couples exclusively to up- and down-type quarks, the charged Higgs contribution to $b \to s\gamma$ transitions constrains its mass to be above $\sim$ 400–500 GeV for $\tan\beta \simeq 1$ [46]. Although our model is not a type-II 2HDM, the $\bar{t}bH^+$ and $\bar{t}sH^+$ couplings are similar, and therefore a comparable bound should be applicable here as well.[1] LHC searches for $H^\pm \to tb$ [47] are sensitive to masses below 250–300 GeV only if $\tan\beta > 2$. As an example, the parameters $\tan\beta = 10$, $v_s = 300$ GeV, $\mu = 181$ GeV, $\lambda_1 = 1$, $\lambda_2 = 0.24$,

[1] As a side remark, we note that the μ parameter cannot be made arbitrarily large while keeping the Higgs mass light, as it would violate unitarity in certain scattering processes. The amplitude for the scattering $\phi_i\phi_h \to \phi_i\phi_j$ would grow like μ^2/m^2, where m is the mass of the virtual scalar exchanged, which would violate unitarity if $\mu \gg m$.

JHEP12(2017)096

$\lambda_s = 2$, $\lambda_3 = 0.1$, $\lambda_4 = 1.5$, $\lambda_{1s} = 1$, and $\lambda_{2s} = 0.1$ lead to a physical Higgs at 125 GeV with couplings almost identical to the SM Higgs (except for small flavor violating couplings to ut and ct), while the two scalars, the pseudoscalar and the charged one would have masses of 620 GeV, 420 GeV, 620 GeV, and 590 GeV. This scalar spectrum would lead to a small deviation on the electroweak T parameter of about $\Delta T = 0.13$.

3 Phenomenology: key constraints

The phenomenology of a light mediator coupled to the standard model fields through kinetic mixing has been studied in the literature in great detail (see ref. [48] and references therein). Our model has a very rich phenomenology as, besides mixing kinetically with the photon, the X gauge boson also mixes with the Z via mass terms. Furthermore, the couplings of X to fermions are flavor non-universal, which would lead to flavor changing neutral currents mediated by both X and the new scalar bosons needed for symmetry breaking. In this section we present the main results obtained from various constraints arising from low energy processes. For definiteness, when quoting numbers we focus on benchmark points where we set $\varepsilon = 0$ and $\tan\beta = 0.5, 2$, while in presenting the constraints as plots we scan the entire allowed range of $\tan\beta = (0.5, 25)$, with $\varepsilon = 0$. We present in table 2 a summary of the most constraining experimental limits together with a brief description of each bound. The branching ratios of X are shown in figure 1, while in figures 2, 4 and 5 we present a summary of the most relevant constraints. Additional experimental constraints are analyzed in section 4, which turn out to be important, but only to a lesser degree. We elaborate now on how the main results summarized in table 2 and figures 2, 4 and 5 are obtained.

3.1 Branching ratios of X

Before discussing the constraints in detail, we first explore the X branching ratios which will define the typical signature of the new gauge boson. If M_X is lighter than the tau mass, it can only decay to first and second family charged fermions, and to all neutrinos. In this case, the partial widths to the charged fermions go as $\sim g_X^2/(1+t_\beta^2)^2$ while the width to $\nu_\tau\nu_\tau$ goes as g_X^2, and hence the branching ratio to the first two families has a t_β^{-4} suppression (in the limit of large t_β). For instance, if $M_X < 2m_\tau$, we obtain

$$\mathrm{BR}(X \to e^+e^-) = \frac{1 - 4s_w^2 + 8s_w^4}{7 - 4s_w^2 + 8s_w^4 + 12t_\beta^2 + 9t_\beta^4} = \frac{0.056}{0.72 + 1.3t_\beta^2 + t_\beta^4}. \tag{3.1}$$

In figure 1 we provide the exact branching ratios of X for two different values of t_β.

To obtain the hadronic partial width for M_X below 1.8 GeV we use the experimentally measured ratio

$$R(s) = \frac{\sigma(e^+e^- \to \text{hadrons}; s)}{\sigma(e^+e^- \to \mu^+\mu^-; s)}, \tag{3.2}$$

JHEP12(2017)096

Experimental constraint	Remarks
K^+ decays	Enhanced $K^+ \to \pi^+ \nu\bar{\nu}$ branching ratio at loop level
B^+ decays	Enhanced $B^+ \to K^+ \nu\bar{\nu}$ branching ratio at loop level. It shows a strong dependence on the mass of the charged scalar
Neutrino oscillations	Non-universal matter effects bounded by atmospheric neutrinos
Atomic parity violation	$X - Z$ mixing modifies weak charge of ^{133}Cs
Υ decay	$\Upsilon \to \gamma X \to \gamma \nu\bar{\nu}$: Goldstone boson equivalence theorem constrains Yukawa coupling
Υ decay	$\Upsilon \to \tau^+\tau^-$: direct constraint on the gauge coupling as the process only involves third family fermions
Electroweak T parameter	$Z - X$ mixing modifies M_Z/M_W and constrains the mixing parameter s_X
$D^0 - \overline{D^0}$ mixing	Mediated by scalar constrains mass of heavy scalar $> O(100)$ GeV; significant constraint on the coupling of X only when X mass is below or close to the D^0 mass
D^+ decays	$D^+ \to \pi^+ X$ contributes to the total D^+ width and to the $\pi^+\ell^+\ell^-$ branching ratio. When the equivalence theorem is valid, this process probes the Yukawa coupling

Table 2. A summary of the major experimental constraints on the model.

where s is the center of mass energy of the e^+e^- collision [49, 50]. We estimate the X hadronic width to be[2]

$$\Gamma(X \to \text{hadrons}) = \Gamma(X \to \mu^+\mu^-) R(s = M_X^2). \tag{3.3}$$

Above 2.2 GeV we calculate the partial widths to partons.

3.2 Lepton universality in Υ decays

Precise measurements of the $\Upsilon \to \tau^+\tau^-$ and $\Upsilon \to \mu^+\mu^-$ branching ratios by BaBar [51] constrain the deviation from lepton universality via the ratio

$$R_{\tau\mu} \equiv \frac{\Gamma(\Upsilon(1S) \to \tau^+\tau^-)}{\Gamma(\Upsilon(1S) \to \mu^+\mu^-)} = 1.005 \pm 0.013(\text{stat.}) \pm 0.022(\text{syst.})\,. \tag{3.4}$$

As the X boson couples dominantly to the third family, this measurement can be used to constrain g_X. In the limit of small $Z - X$ mixing and neglecting the tiny Z exchange diagram, we obtain

$$R_{\tau\mu} \simeq 1 - 2\frac{g_X^2}{e^2}\frac{M_\Upsilon^2}{M_\Upsilon^2 - M_X^2}, \tag{3.5}$$

[2]In fact, the X branching ratios should not be exactly the values obtained here. The hadronic cross section at low energy e^+e^- colliders is dominated by photon exchange. Since the coupling of X to light quarks arrives from $X - Z$ mixing, they differs from the photon couplings: they are not universal and have an axial-vector component. Nevertheless, the hadronic branching ratios derived here are expected to provide a good approximation to the exact ones (which cannot be calculated perturbatively).

JHEP12(2017)096

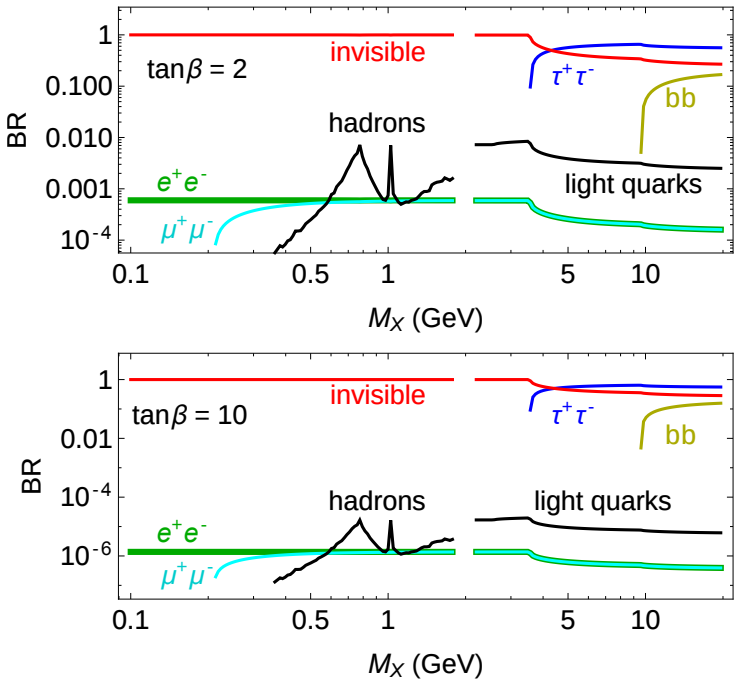

Figure 1. Branching ratios of X for two values of $\tan\beta \equiv v_2/v_1$ with no kinetic mixing.

where the second term comes from the $\gamma - X$ interference. In our numerical evaluation we used the exact expression for $R_{\tau\mu}$. This imposes $g_X < 0.027$ for $m_X \ll m_\Upsilon$. If $m_X \gg m_\Upsilon$, this process actually constrains v_s. In such case, $v_s > 960\,\text{GeV}$, roughly independent of $\tan\beta$.

3.3 $\Upsilon \to X\gamma$ decay

The decay $\Upsilon \to X_L\gamma$ can also occur and can be used to constrain the parameters of the model.[3] Here X_L is the longitudinal mode of X. Although this process involves gauge bosons, the equivalence theorem tells us that this width is actually probing the Yukawa coupling of the corresponding Goldstone to the b quarks, and therefore the bound is independent of whether the theory is gauged or not, as long as $M_X \ll m_b$ holds. Yang's theorem, which states that a vector particle cannot decay into a pair of massless spin-1 particles, does not apply in this case as the Υ is decaying into the longitudinal mode of X and a massless photon. Moreover, due to charge conjugation symmetry, only the axial-vector coupling of X, that is, $c_{bR} - c_{bL}$ from eq. (2.21), will contribute to $\Upsilon \to X_L\gamma$. This branching ratio can be computed using non-relativistic effective field theory [52], where the amplitude is approximated by the zero momentum amplitude for the hard scattering times the wave function of the Υ at the origin, $A_\Upsilon \simeq A(0)\psi(0)$. We get rid of the wave function at the origin by taking the ratio of this width with a measured decay width like

[3] We have checked that $\Upsilon \to X_L X_L$ does not lead to any meaningful bound due to a weaker experimental limit on the branching fraction.

JHEP12(2017)096

$\Upsilon \to e^+e^-$. Therefore we have

$$R \equiv \frac{\mathrm{BR}(\Upsilon \to X_L\gamma)}{\mathrm{BR}(\Upsilon \to e^+e^-)} = \frac{|\psi(0)|^2 \left|A(0; b\bar{b} \to X_L\gamma)\right|^2}{|\psi(0)|^2 \left|A(0; b\bar{b} \to e^+e^-)\right|} \simeq \frac{2g_X^2 v_1^4 m_b^2}{9e^2v^4M_X^2}$$
$$= \frac{2m_b^2 v_1^4}{e^2v^2(v^2v_s^2 + v_1^2v_2^2)} < \frac{4.5 \times 10^{-6}}{0.0238}, \tag{3.6}$$

where the right-hand side of the inequality shows the measured values of the branching ratios being considered [39]. The constraint on v_s is $v_s > 2(0.5)\,\mathrm{TeV}$ for $\tan\beta = 0.5(2)$.

3.4 $D^0 - \overline{D^0}$ mixing

A light gauge boson with flavor changing couplings to quarks can contribute to meson-antimeson mixing. In our model, since the first two families carry no $\mathrm{U}(1)^{(3)}_{B-L}$ charge, and since the third family quark mixings arise from the up-quark mass matrix, these constraints are not severe. The effective interaction mediated by the X gauge boson responsible for $D^0 - \overline{D^0}$ mixing can be written as (see eq. (2.23))

$$\mathcal{L}_{\mathrm{eff}} = C(q^2)(\overline{u}_L\gamma_\mu c_L)^2, \tag{3.7}$$

where

$$C(q^2) = \frac{g_X^2}{9}\frac{|V_{ub}V_{cb}|^2}{q^2 - M_X^2}\,. \tag{3.8}$$

Here q^2 represents the momentum transfer. Demanding that the new contribution does not exceed the experimental value of Δm_D, a limit on $C(m_D^2)$ has been obtained to be [53]

$$C(m_D^2) < \frac{5.9 \times 10^{-7}}{\mathrm{TeV}^2}\,. \tag{3.9}$$

For the case of a light X, this constraint leads to a limit $g_X < 2.6 \times 10^{-2}$, which is significant, but within our range for g_X. When the X boson mass is much larger than m_D, the limit becomes $g_X < 1.4 \times 10^{-2} M_X/\mathrm{GeV}$. The limit is plotted in figure 4 for the full range of M_X.

The Higgs bosons in the model also mediate $D^0 - \overline{D^0}$ mixing. The contribution from tree level neutral scalar exchange to meson oscillations, in general, can be written as [54–56]

$$(\Delta m_S)_\varphi = \frac{1}{3}\frac{f_S^2 m_S B_S}{m_\varphi}\left\{\left[\frac{1}{6}\frac{m_S^2}{(m_{qi}+m_{qj})^2} + \frac{1}{6}\right]\mathrm{Re}\left(h_{ij} + h_{ji}^*\right)^2\right.$$
$$\left. - \left[\frac{11}{6}\frac{m_S^2}{(m_{qi}+m_{qj})^2} + \frac{1}{6}\right]\mathrm{Re}\left(h_{ij} - h_{ji}^*\right)^2\right\}, \tag{3.10}$$

where f_S is the meson decay constant, B_S is the bag parameter, m_S is the meson mass, h_{ij} and m_φ are the couplings to and masses of the physical scalars, and $m_{qi,j}$ are the masses of the quarks constituting the meson. Since the flavor structure is determined, we obtain

$$\Delta m_D^{\mathrm{scalars}} = -2.4 \times 10^{-10}\left(\frac{100\,\mathrm{GeV}}{m_\varphi}\right)^2 \mathrm{Re}\left(\frac{h_{12}^u}{\sqrt{2}m_c/v}\right)^2 \mathrm{GeV}, \tag{3.11}$$

which should be smaller than the theoretical uncertainty of $2.7 \times 10^{-15}\,\mathrm{GeV}$ [39]. As $h_{12}^u \sim \sqrt{2}V_{ub}V_{cb}m_c/v \sim 2 \times 10^{-6}$, the new scalar contributions are within experimental limits, even with the heavy Higgs boson mass m_φ being of order 100 GeV.

JHEP12(2017)096

3.5 $D^+ \to \pi^+ e^+ e^-$ and D^+ lifetime

The flavor properties of X can contribute to the $D^+ \to \pi^+ X \to \pi^+ e^+ e^-$ branching ratio which is bounded to be below 1.1×10^{-6} [39]. This process can be better understood by use of the equivalence theorem, where the Goldstone coupling to uc is given in eq. (2.16). The D^+ to π^+ transition can be parametrized by the form factors

$$\langle \pi^+(p_2)|\bar{u}\gamma_\mu c|D^+(p_1)\rangle = F_+(q^2)(p_1+p_2)_\mu + F_-(q^2)(p_1-p_2)_\mu. \tag{3.12}$$

At low recoils (for $M_X \ll M_{D^+}$), the transition comes entirely from F_+, which can be determined by use of chiral perturbation theory for heavy hadrons (see e.g. ref. [57]),

$$F_+(s) = \frac{f_D}{f_\pi}\frac{g_{D^*D\pi}}{1-s/M_{D^*}^2}. \tag{3.13}$$

Here, $f_D = 200\,\text{MeV}$ and $f_\pi = 130\,\text{MeV}$ are the D^+ and π^+ decay constants, and $g_{D^*D\pi} = 0.59$ is the strong coupling of $D^* \to D\pi$ decay, all yielding $F_+(0) = 0.91$. Numerically, this form factor agrees with the one obtained by assuming vector meson dominance [58]. The $D^+ \to \pi^+ X$ partial width is then given by

$$\Gamma(D^+ \to \pi^+ X) = \frac{1}{144\pi}|F_+(M_X^2)|^2 g_X^2 |V_{ub}|^2 |V_{cb}|^2 \frac{m_{D^+}^3}{M_X^2}. \tag{3.14}$$

Not requiring the e^+e^- pair in the final state makes very hard to reconstruct the D^+ meson as X will typically decay to neutrinos (see figure 1). Nevertheless, one can still constrain the model with the total D^+ width. As a conservative requirement, we demand that the partial width $D^+ \to \pi^+ X$ does not exceed the D^+ total width minus the partial inclusive width to K^0 and $\bar{K}^0$ (to which this new decay does not contribute), that is $\Gamma(D^+ \to \pi X) < 0.39\,\Gamma_{D^+}$ [39]. This constraint is included in our numerical analysis.

3.6 $K^+ \to \pi^+ X$ and $B^+ \to \pi^+ X$

Although the flavor changing couplings in the down-quark sector can be put to zero, one loop corrections will still generate a non-negligible amount of flavor changing. Kaon and B decays are particularly sensitive if the X boson is below the meson mass. More specifically, the loop corrections can contribute to the $K^+ \to \pi^+ X \to \pi^+ \nu\bar{\nu}$ ($B^+ \to K^+ X \to K^+ \nu\bar{\nu}$) branching ratio which is measured to be about 10^{-10} [60, 62] (1.6×10^{-5} [39]). We will discuss the Kaon decay in detail and the results can be promptly generalized for the B decay. As the longitudinal mode of X dominates the contribution, we are interested in the one loop coupling $g_{sdX}(\partial_\mu G_X)\bar{s}\gamma^\mu d$. This calculation differs from the usual Z-induced Kaon decay precisely by the dominance of the longitudinal mode, which lead us to the following considerations. Since the internal X vertex effectively couples to the Yukawa instead of the gauge coupling, we can safely take all quark masses, except for the top, to be zero. The charm quark contribution to the amplitude is suppressed in our scenario, and thus we neglect it. Moreover, the usual counterterms from the self-energy diagrams are omitted since they are proportional to the mass of the s or the b.

JHEP12(2017)096

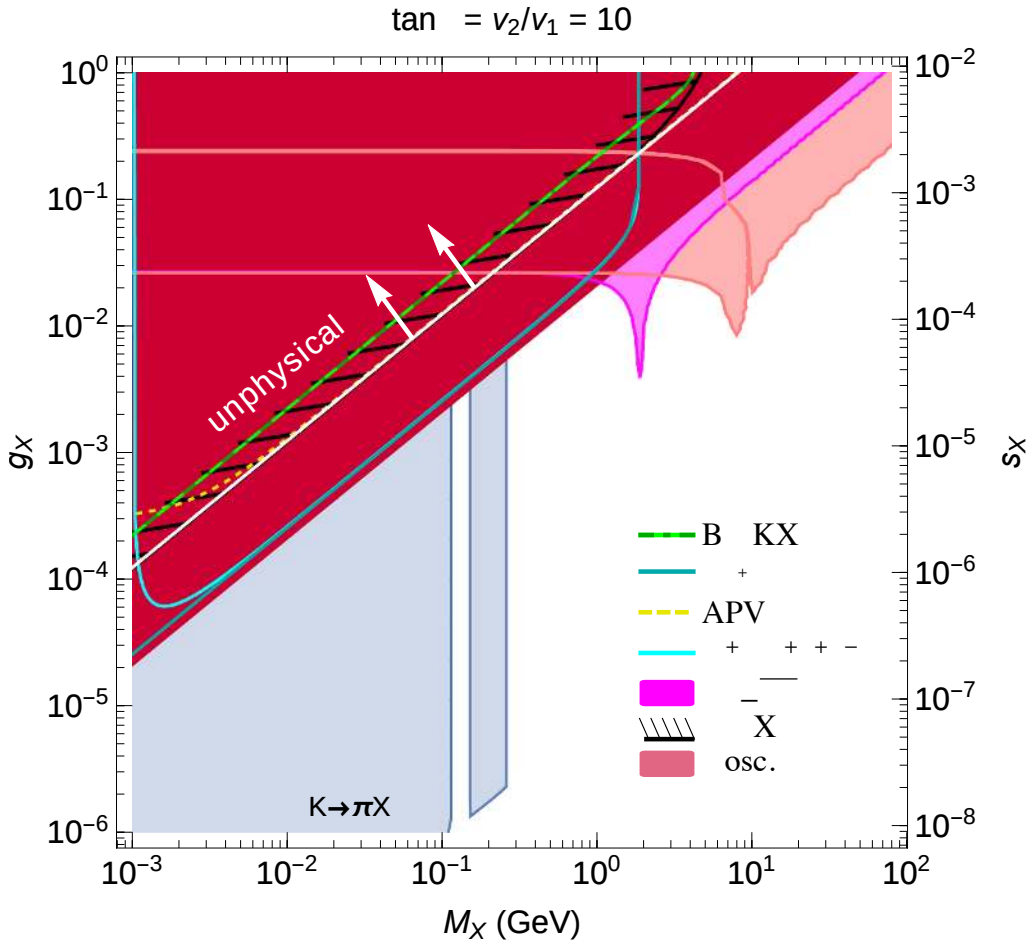

Figure 2. Constraints on the $\mathrm{U}(1)^{(3)}_{B-L}$ gauge boson mass M_X and coupling g_X for $\tan\beta = 10$. For convenience the $X - Z$ mixing, s_X, is also shown. Notice that for a given g_X, the mass of the gauge boson M_X is bounded from below, so there is an unphysical region in the upper left corner of the $M_X \times g_X$ plane (delineated by the white line). The "ν osc." bound comes from non standard interaction effects (matter potential) on atmospheric neutrinos. "APV" refers to atomic parity violation. Here the charged Higgs mass, relevant to the $B \to KX$ constraint, is taken to be 1200 GeV.

There are three main contributions (in the Feynman gauge) to this coupling, i.e., loops with transverse W, longitudinal W or charged Higgs, and both transverse W and charged Higgs (via a $W^{\pm}H^{\mp}G_X$ coupling), see figure 3. For the longitudinal W diagram in figure 3(a), the internal fermions could be tt, or a top and a light up-type quark. These contributions scale as (see eq. (2.16))

$$g^{(1)}_{sdX} \sim \frac{g^2 g_X}{96\pi^2 M_X} \times \{\, V_{td}V^*_{ts}c^2_\beta \;,\; V_{td}(V_{cb}V^*_{cs} + V_{ub}V^*_{us}) \,\} \sim (1.5 - 0.6i)10^{-7}\frac{g_X}{M_X} \times \{-c^2_\beta \;,\; 1\}. \tag{3.15}$$

For the longitudinal W and the charged Higgs in figure 3(b), having a light quark in the loop would suppress the diagram by m^2_{light}/m^2_t, so these contributions are negligible. Thus,

JHEP12(2017)096

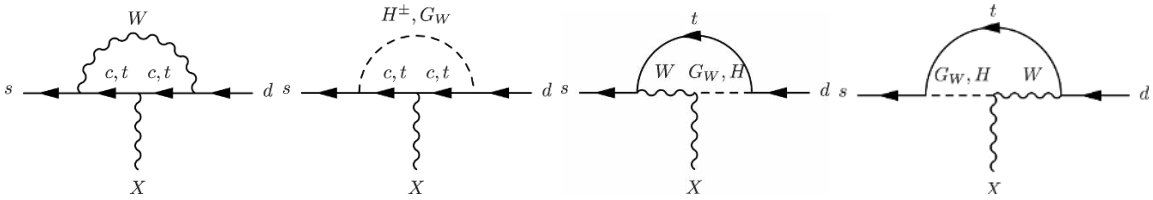

Figure 3. Feynman diagrams involved in the calculation of $K^+ \to \pi^+ X$. Analogous diagrams were computed for $B^+ \to K^+ X$.

the top loop exchange goes as

$$g_{sdX}^{(2)} \sim \frac{g^2 g_X}{96\pi^2 M_X} V_{td} V_{ts}^* \frac{c_\beta^2}{s_\beta} \sim -(1.5 - 0.6i)10^{-7} \frac{g_X}{M_X} \frac{c_\beta^2}{s_\beta}. \tag{3.16}$$

Finally, for the diagram arriving from the $W^\pm H^\mp G_X$ coupling in figure 3(c) and 3(d), only an internal top will lead to sizable contributions,

$$g_{sdX}^{(3)} \sim \frac{g^2 g_X}{96\pi^2 M_X} V_{td} V_{ts}^* c_\beta \sim -(1.5 - 0.6i)10^{-7} \frac{g_X}{M_X} c_\beta. \tag{3.17}$$

We emphasize that all contributions are comparable and have slightly different dependences on t_β, which will result in a bound from $K^+ \to \pi^+ X$ that depends mildly on t_β.

A full calculation of these loop amplitudes yields the following result (for similar calculations see e.g. refs. [63–67])

$$g_{sdX} = i \frac{g^2 g_X}{96\pi^2 M_X} (T_1 + T_2 + T_3), \tag{3.18}$$

$$T_1 = \frac{2t}{(t-1)^2} V_{td} \left[-(V_{cb} V_{cs}^* + V_{ub} V_{us}^*)(t-1)\log t + c_\beta^2 V_{ts}^* (t - 1 - \log t) \right], \tag{3.19}$$

$$T_2 = -\frac{V_{td} V_{ts}^* t\, c_\beta^2}{(t-1)^2 (u-1)^2 s_\beta} \left[s_\beta t (u-1)^2 (1 - t + \log t) + c_\beta u (t-1)^2 (1 - u + \log u) \right], \tag{3.20}$$

$$T_3 = \frac{4 V_{td} V_{ts}^* t\, u\, c_\beta}{(t-1)(u-1)(t-u)} \left[(t-1)\log u - (u-1)\log t \right], \tag{3.21}$$

with $t = m_t^2/M_W^2$ and $u = m_t^2/M_{H^\pm}^2$. The $T_{1,2,3}$ terms correspond to the loop diagrams containing a transverse W, $G_W^\pm$ and $H^\pm$, and the triple coupling $W^\pm H^\mp G_X$, respectively. The amplitude is given by

$$A(K^+ \to \pi^+ X_L) = g_{sdX} \langle \pi | \bar{d} \gamma_\mu s | K \rangle q^\mu \simeq 2 g_{sdX} F_+(0) p \cdot q, \tag{3.22}$$

where the form factor $F_+(0) = 0.96$ [59]. This leads to the partial width

$$\Gamma(K^+ \to \pi^+ X_L) \simeq \frac{1}{16\pi^2} |g_{sdX}|^2 |F_+(0)|^2 M_K^3 \left(1 - \frac{M_\pi^2}{M_K^2} \right)^3, \tag{3.23}$$

where we have neglected M_X^2/M_K^2 terms.

JHEP12(2017)096

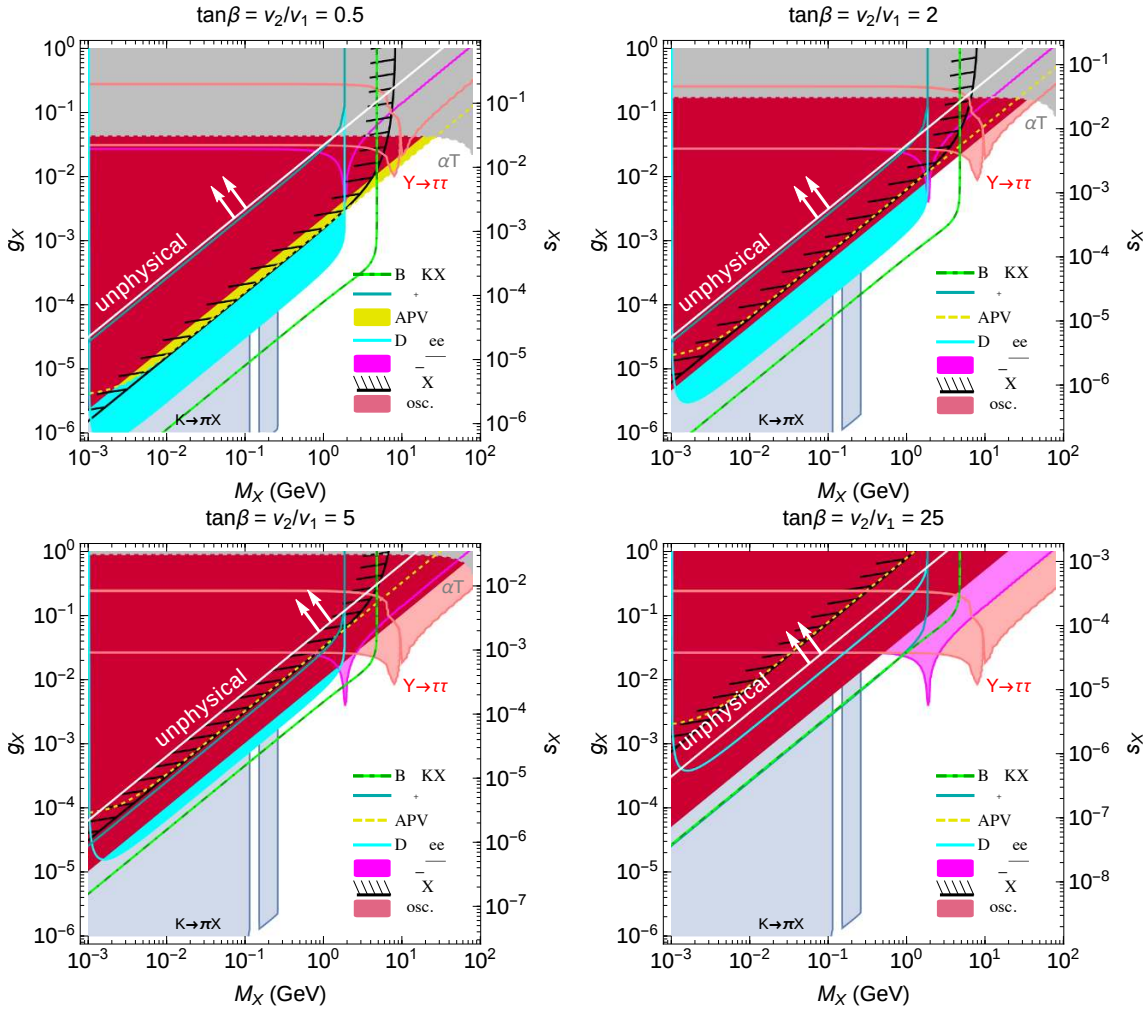

Figure 4. Constraints on the $\mathrm{U}(1)^{(3)}_{B-L}$ gauge boson mass M_X and coupling g_X for $\tan\beta = 0.5, 2, 5, 25$. For convenience the $X - Z$ mixing, s_X, is also shown. Notice that for a given g_X, the mass of the gauge boson M_X is bounded from below, so there is an unphysical region in the upper left corner of the $M_X \times g_X$ plane (delineated by the white line). The "ν osc." bound comes from non standard interaction effects (matter potential) on atmospheric neutrinos. "APV" refers to atomic parity violation.

The two best experimental measurements of $K^+ \to \pi^+ \nu\bar{\nu}$ have different cuts for the pion momentum. In ref. [60], the pion momentum is required to be between 211 and 229 MeV, and the measurement yielded $\mathrm{BR}(K^+ \to \pi^+ \nu\bar{\nu}) = (1.47^{+1.30}_{-0.89}) \times 10^{-10}$, while in ref. [62] the pion momentum is required to be between 140 and 199 MeV and the measurement reads $\mathrm{BR}(K^+ \to \pi^+ \nu\bar{\nu}) = (1.73^{+1.15}_{-1.05}) \times 10^{-10}$. These cuts in momentum translate into the two intervals $M_X < 114\,\mathrm{MeV}$ and $151 < M_X < 260\,\mathrm{MeV}$, where the constraint should be valid. The standard model value for this branching ratio is $(0.80 \pm 0.11) \times 10^{-10}$. The constraint is shown in figures 2 and 4, where we required the sum of the standard and new contributions not to exceed the 2σ experimental value. The gap in the excluded region is the result of the two intervals for M_X.

JHEP12(2017)096

For the $B^+ \to K^+\nu\nu$ decay, a very similar calculation is performed and yields a bound that is weaker than the Kaon decay bound, but goes to higher values of X masses.[4] Furthermore, the dependence with the mass of H^+ and β is more pronounced in the B decay constraint. The reason is because all contributions in eq. (3.19) are comparable for $K^+ \to \pi^+ X$, but only the last one is significant for $B^+ \to K^+ X$, and thus the β dependence and the interplay with eq. (3.21) can lead to cancelations. We have checked numerically that e.g. for $\tan\beta = 5(10)$ such cancelation is possible by having the charged Higgs mass in the range $600 < M_{H^+} < 850\,\text{GeV}$ ($1 < M_{H^+} < 1.5\,\text{TeV}$). In figures 2 and 4 we present the bound from B decays for $M_{H^+} = 1200\,\text{GeV}$.

3.7 Neutrino oscillations

One of the most stringent bounds comes, perhaps surprisingly, from neutrino oscillation experiments. The new interaction will change the neutrino matter potential which modifies the neutrino oscillation pattern. It is useful to express the new interaction in terms of the usual non-standard interaction (NSI) operators which normalize the strength of the new matter potential to that induced by weak interactions. We define the NSI parameter by the operator

$$\mathcal{L}_{\text{NSI}} = 2\sqrt{2} G_F \varepsilon^f_{\alpha\alpha} \left(\bar{\nu}_{\alpha L}\gamma_\mu \nu_{\alpha L}\right)\left(\bar{f}\gamma^\mu f\right), \tag{3.24}$$

and therefore we obtain

$$\varepsilon^f_{\alpha\alpha} = \frac{c_\alpha c_f}{g^2}\frac{4M_W^2}{M_X^2}. \tag{3.25}$$

Due to the lack of flavor universality of the new gauge group we expect a non-standard matter potential (we remind the reader that a universal diagonal matter potential has no impact on neutrino oscillations)

$$V_X \propto \text{diag}\,(0, \quad 0, \quad \varepsilon_{\tau\tau})\,. \tag{3.26}$$

It is important to mention that, as normal matter is neutral, the kinetic mixing parameter ε does not play any role in neutrino oscillations. If we assume the number density of protons, neutrons and electrons all to be the same, and use eqs. (2.21) and (3.25), we can translate the non-universal matter effects into the usual non-standard interaction parameter:

$$\begin{aligned}\varepsilon_{\tau\tau} &\equiv \varepsilon^p_{\tau\tau} + \varepsilon^n_{\tau\tau} + \varepsilon^e_{\tau\tau} \\ &= \frac{4M_W^2}{g^2 M_X^2}(-g_X)\left[c_{eR} + c_{eL} + 3(c_{uR} + c_{uL} + c_{dR} + c_{dL})\right] = 3\frac{v_1^2 v^2}{v_1^2 v_2^2 + v_s^2 v^2}.\end{aligned} \tag{3.27}$$

Atmospheric neutrinos play a major role in constraining the $\tau\tau$ NSI, leading to [68]

$$|\varepsilon_{\tau\tau}| < 0.09. \tag{3.28}$$

Notice that the new matter potential does not depend on the gauge coupling, but only on the VEVs of the scalar fields, analogous to what happens with the standard matter potential. Note also that in the absence of the singlet scalar s, the non-standard interaction would be $\varepsilon_{\tau\tau} = 3v^2/v_1^2 > 3$, which violates the experimental limit of eq. (3.28), for any M_X. Plugging in numbers we find $v_s > 1.3(0.6)\,\text{TeV}$ for $\tan\beta = 0.5(2)$.

[4] For the $B \to K$ transitions, the relevant form factor is smaller, $F_+(0) = 0.331$ [61].

JHEP12(2017)096

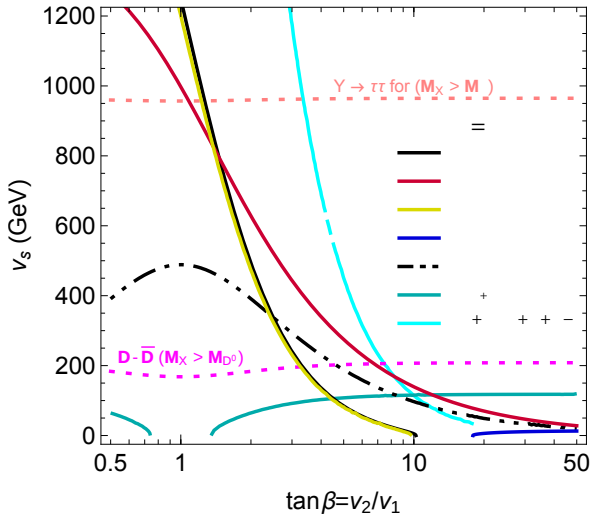

Figure 5. Constraints on the VEV of the SM singlet scalar s as a function of $\tan\beta \equiv v_2/v_1$ from $\Upsilon \to X_L\gamma$ decay, atomic parity violation (APV), $D^+ \to \pi^+\mu^+\mu^-$, total D^+ width, neutrino oscillations, top quark total width, and Higgs invisible decays (see section 4). We also show the bounds on v_s from $\Upsilon \to \tau^+\tau^-$ and $D^0 - \overline{D^0}$ mixing, although they only apply for $M_X \gg M_\Upsilon$ and $M_X \gg M_{D^0}$, respectively (see figure 2 and 4).

3.8 Electroweak T parameter

From the mass matrix (2.10), we can see that the Z boson mass is shifted from its SM value by

$$\Delta M_Z^2 \simeq \frac{g_X^2}{9}\frac{v_1^4}{v^2}, \tag{3.29}$$

which contributes to the electroweak T parameter. Therefore, the current bound [39][5]

$$T \simeq \frac{1}{\alpha}\frac{\Delta M_Z^2}{M_Z^2} = 0.01 \pm 0.12 \tag{3.30}$$

imposes a constraint $g_X < 0.035$ for $\tan\beta = 1/2$, with the constraint becoming weaker for larger values of $\tan\beta = v_2/v_1$ as the fourth power.

The constraints derived here are plotted in the $g_X - M_X$ plane in figure 2 and 4. The origin of various constraints are labeled. The four panels correspond to four values of $\tan\beta = v_2/v_1$. The label on the right indicates the $Z - X$ mixing angle s_X. Note that some regions in this plane are excluded theoretically, since M_X must obey an inequality.

We present in figure 5 the constraints from Υ, D^+, top and Higgs decays (see section 4), atomic parity violation, neutrino oscillations and $D^0 - \overline{D^0}$ mixing on v_s as a function of $\tan\beta$. We do not show the $K^+ \to \pi^+ X$ bound, but we notice that it is much stronger than the others for $M_X < 114\,\text{MeV}$ and $151 < M_X < 260\,\text{MeV}$. Also, the $B^+ \to K^+ X$ is omitted due to the strong dependence with M_{H^+}. Outside the Kaon bound region, we see clearly that $D^+ \to \pi^+ e^+ e^-$ dominate for $\tan\beta < 8$, as long as $M_X < m_{D^+} - m_{\pi^+}$. The total D^+ width dominates for $\tan\beta > 13$ if $M_X < m_{D^+} - m_{\pi^+}$. The neutrino oscillations bound

[5] X is not expected to contribute to the running of electroweak parameters at low scales due to small g_X.

JHEP12(2017)096

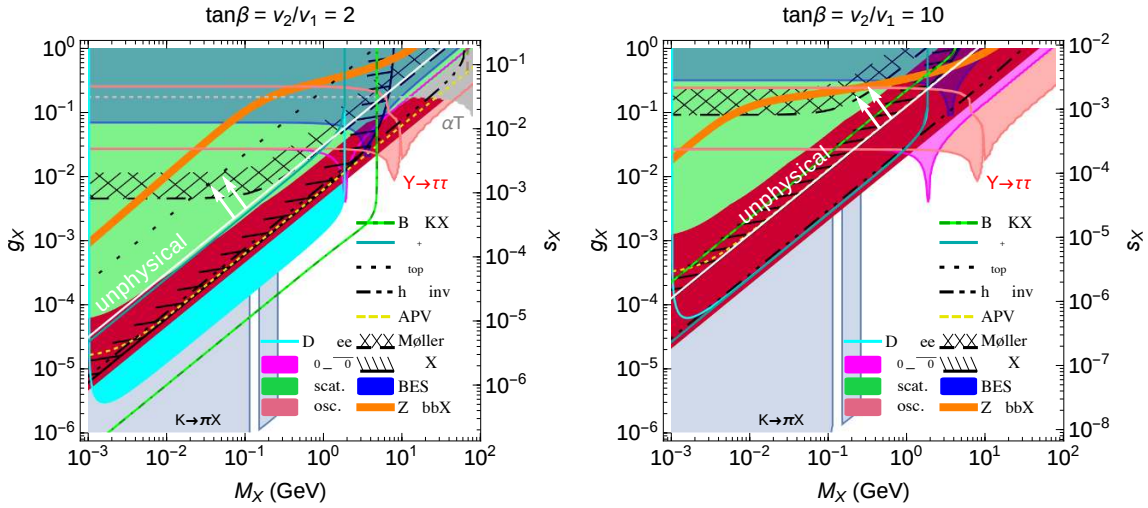

Figure 6. More complete list of constraints on the $\mathrm{U}(1)^{(3)}_{B-L}$ gauge boson mass M_X and coupling g_X for $\tan\beta = 2, 10$. For convenience the $X - Z$ mixing, s_X, is also shown. Notice that for a given g_X, the mass of the gauge boson M_X is bounded from below, so there is an unphysical region in the upper left corner of the $M_X \times g_X$ plane (delineated by the white line). The "ν scat" bound is a combination of all neutrino scattering experiments listed in the text, while "ν osc." comes from non standard interaction effects (matter potential) on atmospheric neutrinos. "APV" refers to atomic parity violation. Here the charged Higgs mass, relevant to the $B \to KX$ constraint, is taken to be 1200 GeV.

is independent of M_X. It is the main constraint for $8 < \tan\beta < 13$, or $1.5 < \tan\beta$ if the D^+ channels are forbidden. The region $\tan\beta < 1.5$ is well covered for any M_X by the combination of APV and $\Upsilon \to X\gamma$. Higgs invisible branching ratio and top width provide complementary constraints for large $\tan\beta$. Once the X boson mass exceed M_{D^0} or M_Υ, $D^0 - \overline{D^0}$ mixing and $\Upsilon \to \tau\tau$ dominate the constraints for $\tan\beta$ above 7.5 and 3.2, respectively.

4 Other constraints

Here we provide a more complete analysis, including those constraints which turned out *a posteriori* to be not as stringent as the ones discussed in the previous section. In figure 6 we present the bounds from the previous section together with a few bounds from this section (chosen by their importance in ruling out the physical region of the parameter space). In table 3 we list the additional constraints on the model presented in this section.

4.1 Atomic parity violation

An important process is atomic parity violation (APV), in which the weak charge, especially for ^{133}Cs, has been measured very precisely. The standard model prediction is $Q_W^{\mathrm{SM}} = -73.16 \pm 0.3$, while the experimental measurement combined with theoretical calculations yield $Q_W = -73.16 \pm 0.35$ [69]. In our model, since the X boson mixes with the Z, there are new contributions to Q_W. The fractional contribution of the X mediated

JHEP12(2017)096

Experiment	Constraint
Møller scattering	$Z - X$ mixing leads to parity violation in e^-e^- scattering
$t \to cX$	Flavor changing ctX coupling can contribute to the total top width, which is bounded as $\Delta\Gamma_t < 0.44\,\text{GeV}$ [39]
$Z \to f\bar{f}X$	There is no dedicated search for $Z \to \tau^+\tau^- + \not{E}_T$ ($Z \to b\bar{b} + \not{E}_T$). A direct bound on g_X may be obtained by requiring these branching ratios not to exceed 0.2 MeV (2.8 MeV).
$h \to XX$	Decays to longitudinal X pair contributes to invisible width.
X at the LHC	Resonant production of X decaying to $\tau^+\tau^-$ in association with two b-jets at the LHC may constrain the parameter space for realizations of the model at the TeV scale
Fixed target	Much weaker than in kinetic mixing scenario [78] as $\text{BR}(X \to \nu\nu)$ typically dominates, especially for large $\tan\beta$.
$(g-2)_e$ and $(g-2)_\mu$	The axial-vector contribution does not saturate for small M_X [79, 80], but the bound is nevertheless weak.
BESIII	$e^+e^- \to \tau^+\tau^-$ near the τ threshold [81].
K, B_d, B_s oscillation	May lead to strong bounds on off-diagonal Yukawa couplings, forcing V_{CKM} to be generated in the up sector. The contribution from heavy scalar exchange is both loop and CKM suppressed.
Neutrino scattering	Borexino [8, 82], GEMMA [83], CHARM II [30, 84], TEXONO [85], MiniBooNe [86, 87], and LSND [88] constrain $\nu - e$ scattering. NUTEV data displays a 2.7σ tension with the SM prediction [89]. We require this tension not to be worsened by 1.6σ.
$W \to \tau\nu X$	For $M_X \ll M_W$ probes the Yukawa coupling to τ, but does not constrain the model significantly.
$t \to bWX$	For $M_X \ll m_t$ probes the Yukawa coupling to the top, but does not constrain the model significantly.
LEP	LEP bound on resonant $e^+e^- \to \tau^+\tau^-$ production [90] can be used to put bounds on the X coupling to leptons.
$\pi \to X\gamma$	The bound derived in the case of pure kinetic mixing [91] can be easily translated to our scenario, leading to a very weak bound in the whole parameter space.

Table 3. List of constraints on the $\text{U}(1)^{(3)}_{B-L}$ gauge and scalar sector. For the neutrino scattering bounds, the approximation of mean momentum transfer $\langle q^2 \rangle$ was made separately for each experiment. See section 4 for details.

APV is given by

$$f_{\text{APV}} = 1 + s_X^2 \frac{M_Z^2}{M_X^2 + q^2} = 1 \pm 0.0063, \tag{4.1}$$

where $\langle q^2 \rangle \simeq (2.4\,\text{MeV})^2$ is the estimated average squared momentum transfer. This allows us to put a direct bound $v_s > 2(0.5)\,\text{TeV}$ at 90% CL for $\tan\beta = 0.5(2)$ and for mediator squared-masses above $\langle q^2 \rangle$.

JHEP12(2017)096

4.2 Flavor changing top decay

The X boson can also mediate flavor-changing processes involving the top quark. The decay $t \to cX$ is predicted in the model. The width for this decay can be calculated directly, or using the equivalence theorem and the Goldstone boson coupling eq. (2.16),

$$\Gamma(t \to cX) \simeq \frac{g_X^2}{288\pi} \frac{|V_{cb}|^2 m_t^3}{M_X^2}. \tag{4.2}$$

For $g_X = 10^{-3}$ and $M_X = 100\,\text{MeV}$, the width is 0.9 MeV, corresponding to a branching ratio of 6.5×10^{-4}, which would not be easy to observe. However, if the mass of X is lower, this branching ratio increases. For example, when $M_X = 1\,\text{MeV}$, top quark width would set a constraint on g_X to be less than about 2×10^{-4}. The new contribution to the top quark width cannot exceed 0.38 GeV (at 2 sigma) [39]. The top width provides a direct bound v_s, which turns out to be important only for large values of $\tan\beta$ (see figure 5). Note that this decay can be understood in terms of Goldstone boson equivalence theorem, as the top decays primarily into the longitudinal X. Apart from $t \to cX$, as the Higgs has flavor changing couplings (see eq. (2.29)), $t \to ch$ transitions are also possible. Nevertheless, the flavor changing Yukawa is doubly suppressed, by V_{cb} and by the small mixing angle between H and H', making this branching ratio typically small, below 10^{-4}.

4.3 $h \to XX$ decay

The presence of $X - Z$ mixing will lead to Higgs decays to X pairs (dominantly to the longitudinal modes). The X bosons typically further decay to neutrinos, thus leading to a contribution to the invisible Higgs branching ratio which is bounded to be smaller than 0.28 [70]. The invisible width is given by (see eq. (2.32))

$$\Gamma(h \to XX) = \frac{g_X^4}{2592\pi} \frac{v_1^4 v_2^4}{v^6 M_h} \left(\frac{M_h^4 - 4M_X^2 M_h^2 + 12 M_X^4}{M_X^4} \right) \sqrt{1 - \frac{4M_X^2}{M_h^2}}. \tag{4.3}$$

In the limit of $M_X \ll M_h$ this becomes

$$\Gamma(h \to XX) = \frac{M_h^3 \sin^4(2\beta)}{32\pi v^2 [\sin^2(2\beta) + 4v_s^2/v^2]^2}, \tag{4.4}$$

which translates to $v_s > \sin(2\beta) \times 490\,\text{GeV}$. Notice that the Higgs can also decay to XZ via the mixing with $\text{Re}(s)$, leading to interesting modifications of Higgs phenomenology (e.g. $h \to XZ \to \tau^+\tau^-\ell\ell$, with the τ pair invariant mass at M_X^2). Nonetheless, since this mixing is a free parameter, we do not consider this channel.

4.4 Møller scattering

Measurements from SLAC E158 [71] are sensitive to modifications of the parity-violating asymmetry in low scale e^-e^- scattering,

$$A_{\text{PV}} = \frac{\sigma_R - \sigma_L}{\sigma_R + \sigma_L} = (-175 \pm 30_{\text{stat}} \pm 20_{\text{syst}}) \times 10^{-9}, \tag{4.5}$$

JHEP12(2017)096

where $\sigma_{R,L}$ indicate the cross section for incident right- and left-handed electrons. The asymmetry is dominated by the interference term between the photon and the Z. In this experiment, the sensitivity to s_w^2 is significantly enhanced due to an accidental cancelation in the factor $(1/4 - s_w^2)$ appearing in the asymmetry. In our model, this cancelation plays no role in the sensitivity to the X boson contributions, as the parity-violating coupling comes entirely from the mixing with the Z. Because of that, the X fractional contribution to $A_{\rm PV}$ is basically the mixing with the Z and the ratio of propagators,

$$\frac{A_{\rm PV}^{\rm SM+X}}{A_{\rm PV}^{\rm SM}} - 1 = \frac{s_X^2 M_Z^2}{q^2 + M_X^2} < 0.21, \tag{4.6}$$

where we added the statistical and systematical fractional errors in quadrature. The average momentum transfer is $\langle q^2 \rangle = (0.161\,\text{GeV})^2$.

4.5 Z decays to $\tau^+\tau^- X$ and $b\bar{b}X$

For M_X below the Z mass, the processes $Z \to \tau^+\tau^- X$ and $Z \to b\bar{b}X$ may also constrain our model. When $M_X \ll M_Z$, these processes will measure the diagonal Yukawas between the third family fermions and G_X, the Goldstone mode of X, see eq. (2.16).

In this limit, the partial widths above can be written as[6]

$$\Gamma(Z \to f\bar{f}X) = \frac{N_c}{192\pi^3} M_Z |y_f^{G_X}|^2 \left[g_V^{f\,2} \left(1 + \log\frac{M_Z^2}{M_X^2}\right) + g_A^{f\,2} \left(-\frac{14}{3} + \log\frac{M_Z^2}{M_X^2}\right)\right], \tag{4.7}$$

with

$$g_V^\tau = \frac{g}{4c_w}(4s_w^2 - 1), \quad g_A^\tau = \frac{g}{4c_w}, \quad g_V^b = \frac{g}{4c_w}\left(\frac{4s_w^2}{3} - 1\right), \quad g_A^b = \frac{g}{4c_w}. \tag{4.8}$$

In the limit of heavy X, the Goldstone modes contribute very little, and the mass of the fermions can be safely neglected. In this case, the results of ref. [72] on $Z \to W\ell\nu$ can be easily recast into our scenario leading to

$$\frac{d\Gamma(Z \to f\bar{f}X)}{dx} = \frac{M_Z}{6\pi^3}\left[\left(g_V^f c_V^f + g_A^f c_A^f\right)^2 (h_1(x) + h_3(x))\right], \tag{4.9}$$

where $x = 2E_X/M_Z$ is the energy fraction carried by X, and

$$c_V^f \equiv (c_{fR} + c_{fL}), \quad c_A^f \equiv (c_{fR} - c_{fL}), \tag{4.10}$$

where c_α is defined in eq. (2.21). The functions $h_1(x)$ and $h_3(x)$ are given in eqs. (10.1), and (10.3) of ref. [72]. The total width is obtained by integrating the differential width in x from $2M_X/M_Z$ to $1 + M_X^2/M_Z^2$.

There are no dedicated searches for these channels. For the $Z \to \tau^+\tau^-$, we require the additional width not to exceed the experimental uncertainties of 0.2 MeV. In the case of $Z \to b\bar{b}$, the uncertainty on R_b imposes the additional width to be below 2.8 MeV. In figure 4 we show only the constraint from $Z \to b\bar{b}X$, as it is slightly more stringent than

[6] The log divergence should be regulated by the 1-loop amplitude. We estimate the effect to be small for the range of parameters chosen here.

JHEP12(2017)096

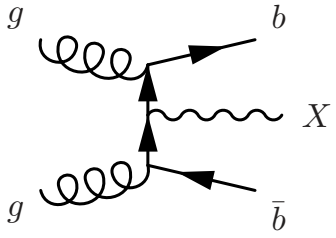

Figure 7. Dominant X production mode at the LHC for m_X at the TeV scale.

$Z \to \tau^+\tau^- X$. These effects could be of particular interest to the models discussed in refs. [21, 22]. It would also be interesting to search for such a light gauge boson in the decay of Z, since the new decay mode can be distinguished from the two-body decay mode $Z \to f\bar{f}$ by its distinct kinematic shape.[7]

4.6 *X* resonant production at the LHC

If the X boson is above the electroweak scale, the LHC will eventually provide the best bound on the direct production of X. The T parameter imposes the mixing with the Z to be small, and therefore the couplings of a heavy X-boson to the third family fermions will dominate the phenomenology. Although a comprehensive LHC analysis is beyond the scope of this paper, we point out that a search for a resonance decaying to $\tau^+\tau^-$ in association with two b-jets seems to be a promising way of exploring this model, see figure 7. In fact, the $b\bar{b}\tau^+\tau^-$ final state has been studied by CMS [73] and ATLAS [74] in third generation leptoquark searches, but since each $b\tau$ pair reconstructs a resonance it is not straightforward to interpret these results in the context of our model.

Should the X gauge boson have already shown up in the dimuon searches at the LHC? At 13 TeV LHC, the cross section for $b\bar{b}$ production is about 154 micro-barn. The X boson may be emitted from the b quark. We estimate the production cross section for $pp \to b\bar{b}X$ to be $\sim 154\mu\text{b} \times g_X^2/(36\pi)$. For $g_X = 0.05$, number of X bosons produced with $40\,\text{fb}^{-1}$ of data is about 10^8. The branching ratio for $X \to \mu\mu$ is about 10^{-3} (10^{-6}) for $\tan\beta = 2(10)$, which would imply that the number of dimuon events is about 10^5 (10^2). The background for dimuon resonance searches is a few times 10^5 events per GeV at low mass, and thus the X boson would not have been observed. With more data, for a range of model parameters, the X boson may be observable at the LHC as a dimuon resonance.

4.7 Meson-antimeson oscillations

The presence of FCNC in scalar and gauge boson interactions can modify $K^0 - \overline{K^0}$, $B_d - \overline{B}_d$, $B_s - \overline{B}_s$, and $D^0 - \overline{D^0}$ oscillations. The case of $D^0 - \overline{D^0}$ mixing, which provides the best limits on the model, is already analyzed in section 3. Here we complete this analysis.

The general scalar contributions to meson-antimeson mixing is given in eq. (3.10). The vector boson X will also contribute to the meson oscillation via s-channel exchange [75]

$$(\Delta m_S)_X = \frac{\sqrt{2}}{6} G_F f_S^2 m_S B_S \eta_S \frac{M_Z^2}{m_S^2 - M_X^2} \left| \frac{2 g_X^2 U_{ij}^X / 3}{g/c_w} \right|^2 , \tag{4.11}$$

[7] We thank A. Khanov for discussion on this prospects.

JHEP12(2017)096

where $U^X = V^L_{u,d}.\mathrm{diag}(0,0,1).V^{L\dagger}_{u,d}$. In fact, this contribution is suppressed by both the small mixing, U^X_{ij} and g_X. Except for the case of $D^0 - \overline{D^0}$ mixing where the X boson exchange becomes important for $M_X \sim$ MeV, this contribution is generally sub-leading.

Using the parameters found in refs. [54, 55] and imposing that the extra contribution is smaller than the experimental and theoretical uncertainties [76, 77] we find that

$$K - \bar{K}: \quad \left(\frac{100\,\mathrm{GeV}}{m_\varphi}\right) \mathrm{Re}\left(\frac{h^d_{21}}{\sqrt{2}m_s/v}\right) \lesssim 1.4 \times 10^{-2} \tag{4.12}$$

$$B_d - \bar{B}_d: \quad \left(\frac{100\,\mathrm{GeV}}{m_\varphi}\right) \mathrm{Re}\left(\frac{h^d_{31}}{\sqrt{2}m_b/v}\right) \lesssim 3.1 \times 10^{-3} \tag{4.13}$$

$$B_s - \bar{B}_s: \quad \left(\frac{100\,\mathrm{GeV}}{m_\varphi}\right) \mathrm{Re}\left(\frac{h^d_{32}}{\sqrt{2}m_b/v}\right) \lesssim 1.3 \times 10^{-2} \tag{4.14}$$

$$D - \bar{D}: \quad \left(\frac{100\,\mathrm{GeV}}{m_\varphi}\right) \mathrm{Re}\left(\frac{h^u_{12}}{\sqrt{2}m_c/v}\right) \lesssim 3.4 \times 10^{-3} \tag{4.15}$$

In our benchmark points, all contributions to down flavored meson oscillation vanish, since V_{ub} and V_{cb} are generated in the up-quark sector.

4.8 Tau physics

Precise measurements of the τ mass and production cross section were performed by the BESIII collaboration [81]. Doing a scan in the energy of the e^+e^- beam around the τ threshold made it possible to measure the $\tau\tau$ production cross section at the sub-percent level. To estimate the constraint from BESIII, we require the ratio of BSM and standard cross sections $\sigma(e^+e^- \to A, X, Z \to \tau^+\tau^-)/\sigma_{\mathrm{SM}}(e^+e^- \to A, Z \to \tau^+\tau^-)$ not to exceed the experimental errors at fixed $\sqrt{s}$, namely 3.1039, 3.542, 3.553, and 3.5611 GeV.

4.9 $(g-2)_\mu$

The X boson may contribute to the muon anomalous magnetic moment through its mass mixing with the Z. In contrast to the case of pure vectorial couplings, the axial-vector contribution to $(g-2)_\mu$ does not saturate for small M_X [79, 80], growing as M_X diminish. For $M_X \ll m_\mu$, requiring the modification to a_μ not to exceed 10.8×10^{-8} the constraint is approximately

$$g_X < 1.2 \times 10^{-4}(1 + \tan^2\beta)\left(\frac{M_X}{\mathrm{MeV}}\right) \qquad \text{from } (g-2)_\mu. \tag{4.16}$$

Nevertheless, for a given M_X the g_X coupling is bounded from above by (see eq. (2.14))

$$g_X < 1.2 \times 10^{-5}\left(\frac{1 + \tan^2\beta}{\tan\beta}\right)\left(\frac{M_X}{\mathrm{MeV}}.\right) \qquad \text{from eq. (2.14)}, \tag{4.17}$$

Thus, for any reasonable value of $\tan\beta$, the bound from the muon anomalous magnetic moment is always in the "unphysical" region of figure 5.

JHEP12(2017)096

4.10 Neutrino-electron scattering

The neutrino electron scattering cross section may be considerably modified in the presence of the extra gauge boson X_μ. We have estimated the constraint coming from a given experiment by making the simplified assumption of a fixed momentum transfer. Due to the large number of experiments, we only state the numbers we use. All limits can be found in figure 4.

The limits from solar neutrino measurements at the Borexino experiment [82] were calculated in ref. [8] for the universal $B-L$ scenario. In our case, we estimated it by requiring that the $\nu - e$ scattering cross section does not exceed 10% of the standard cross section for $q^2 = 2m_e E_{\rm rec}$, where m_e and $E_{\rm rec} \sim 300\,{\rm keV}$ are the electron mass and recoil energy. Limits coming from reactor neutrinos at the GEMMA experiments [83] were also calculated for a universal $B-L$ light gauge boson in ref. [8]. We have checked that in the MeV $-$ GeV region, the GEMMA experiment is always less sensitive than Borexino.

The bound from CHARM II [84] was computed for the case of NSI in ref. [30], yielding

$$-0.025 < \varepsilon^{eL}_{\mu\mu} < 0.03, \qquad -0.027 < \varepsilon^{eR}_{\mu\mu} < 0.03. \tag{4.18}$$

This can be easily translated to our case using eq. (3.25) and fixing $q^2 = 0.01\,{\rm GeV}^2$.

The TEXONO experiment [85] measured $\bar{\nu}_e$ scattering on electrons in a CsI detector with $q^2 \approx 3\,{\rm MeV}^2$. The ratio of the experimental cross section to the SM one was found to be

$$\frac{\sigma_{\rm exp}}{\sigma_{\rm SM}} = 1.08 \pm 0.21({\rm stat}) \pm 0.16({\rm syst}). \tag{4.19}$$

There are two other measurements of the TEXONO experiment using a high purity Ge detector [92] and a N-type point-contact Ge detector [93]. We have checked that these bounds are negligible for X at or above the MeV scale.

The MiniBooNe experiment [86, 87] has measured a variety of neutrino cross sections, ranging from ν_μ neutral current scattering on nucleus to $\nu_e - e$ elastic scattering. Due to the mass dependence, scattering on electrons will have a lower q^2 for the same recoil energy and thus will be more important for a lighter mediator. We assumed conservatively $q^2 = 2m_e E_{\rm th}$, where $E_{\rm th} = 140\,{\rm MeV}$ is the experimental threshold energy of the scattered electron, and a 10% error on the elastic cross section.

The NUTEV experiment measured the ratio of neutral to charged current cross sections for ν and $\bar{\nu}$ to 1% precision and with a mean $\langle q^2 \rangle \approx -20\,{\rm GeV}^2$ [89]. In fact, the NUTEV measurement of $(g_L^{\rm eff})^2$ displays a tension with the standard model prediction at the 2.7σ level (see ref. [89] for details). A positive g_X enhances this cross section making the tension worse. We use the NSI bound from ref. [30], namely,

$$|\varepsilon^q_{\mu\mu}| < 0.003, \quad q = u, d. \tag{4.20}$$

Finally, the measurement of the $\nu - e$ elastic scattering cross section, with a $\sim 17\%$ precision, by LSND [88] can also be used to constrain non-standard interactions in the neutrino sector [30]. In the light mediator scenario, the LSND bound is somewhat special due to its low threshold for the electron recoil energy, $E_{\rm th} = 18\,{\rm MeV}$. The limits found in ref. [30] can be applied to our scenario by using eq. (3.25) with $q^2 = 2m_e E_{\rm th}$.

JHEP12(2017)096

4.11 $t \to bWX$

Another 3-body decay that can be enhanced by the Goldstone coupling is $t \to bWX$. The dominant contribution comes from the X emission by the initial top quark. The differential width is given by

$$\frac{d\Gamma(t \to bWX)}{dxdy} = \frac{g^2}{128\pi^3} m_t \left(\frac{g_X}{3}\frac{m_t}{M_X}\frac{v_1^2}{v^2}\right)^2 \frac{J}{(2-2(x+y)^2-r_X)^2+r_\Gamma}, \tag{4.21}$$

where $x \equiv E_W/m_t$ and $y \equiv E_b/m_t$ are the energy fractions carried by the W and the b quark,

$$J = (4x-1)(x+y-1) + r_W(2-x-3y) + \frac{1}{r_W}(2y-1)\left[2x^2+x(4y-3)+2y^2-3y+1\right], \tag{4.22}$$

and we define $r_X \equiv M_X^2/m_t^2$, $r_W \equiv M_W^2/m_t^2$, and $r_\Gamma = \Gamma_t^2/m_t^2$, with Γ_t being the top width of 1.41 GeV. The mass of the b quark was neglected. To obtain the total width, the integration should be performed within

$$\sqrt{r_W} \le x \le (1+r_W)/2, \tag{4.23}$$

$$(1-x-\sqrt{x^2-r_W})/2 \le y \le (1-x+\sqrt{x^2-r_W})/2. \tag{4.24}$$

For $M_X = 1\,\text{MeV}$ and $\tan\beta = 1$, requiring the additional width not to exceed the total top width uncertainty of 0.38 GeV yields $g_X < 1.1 \times 10^{-3}$.

4.12 $W \to \tau\nu X$

Similar to the $Z \to f\bar{f}X$ decay, the W can decay to $\tau\nu X$, where the longitudinal X dominates for low masses. The width is given by

$$\Gamma(W \to \tau\nu_\tau X) = \frac{N_c\, g^2}{1536\pi^3} M_W \left(\frac{g_X}{3}\frac{m_\tau}{M_X}\frac{v_1^2}{v^2}\right)^2 \left(-\frac{11}{6} + \log\frac{M_W^2}{M_X^2}\right). \tag{4.25}$$

Notice that the coupling proportional to $B-L$ does not have the longitudinal enhancement. The decay proceeds through $Z - X$ mixing. The X typically decays to neutrinos, so the signature would still be $\tau + \not{E}_T$, but with a distinct p_T^τ distribution. Since there is no dedicated search for such signature, we demand the width not to exceed 20 MeV, the uncertainty on the $W \to \tau\nu$ partial width. The bound is nevertheless weak: for $M_X = 1\,\text{MeV}$ and $\tan\beta = 2$ it leads to $g_X < 0.01$.

5 Outlook

Inspired by the anomaly cancelation within a single standard model generation and the fact that the third generation appears different with heavy masses and small mixings with the first two generations in the quark sector, we have proposed and analyzed a gauged $\text{U}(1)^{(3)}_{B-L}$ symmetry that acts only on the third family. We have constructed a class of fully consistent flavor models below the weak scale, which is renormalizable and exhibits a light gauge boson that couples non-universally to the quark and lepton flavors.

JHEP12(2017)096

Our model exhibits a very rich phenomenology, yielding many interesting observables of different types. For instance, to accommodate the observed mixing of generations in the presence of the new flavor-dependent U(1) gauge symmetry it is necessary to extend the Higgs sector. The minimal extension involves a second Higgs doublet (for the mixing) as well as an additional SM singlet which is charged under this U(1), for consistent symmetry breaking and phenomenology. While two Higgs doublet models, with or without additional singlets, have been extensively studied in the literature, our realization has a number of unique features due to the unusual flavor structure. The extended Higgs sector of this model can be studied at the LHC, as well as with precision electroweak data and flavor observables. Here, we only sketched the relevant bounds; an in-depth analysis will be desirable.

Another class of relevant observables that is sensitive to the structure of the extended Higgs sector is based on precision meson decay data. This includes $K^+ \to \pi^+ X$, $B^+ \to K^+ X$, $t \to cX$, $\Upsilon \to X\gamma$, $D^+ \to \pi^+ X$ decays, among others. For decay processes, at high energies, the equivalence theorem implies that the longitudinal mode can be replaced by the Goldstone boson associated with the breaking of the symmetry. Thus, many of the constraints would survive even in the limit of a global symmetry. When the decay channel $K^+ \to \pi^+ X$ is kinematically viable, kaon physics poses by far the most important bound on the model. $B^+ \to K^+ X$ is also quite stringent, but depends strongly on M_{H^+} and $\tan\beta$.

When X is heavier, for a range of parameters with $g_X \sim 10^{-3}$–10^{-2} and the X gauge boson mass of order 300 MeV–1 GeV, neutrino oscillations become the main probe even at present. The induced neutrino non-standard interaction is flavor conserving, namely $\epsilon_{\tau\tau}$ in the present model, and its values are in the interesting range for DUNE, Hyper-Kamiokande, PINGU, and other present and future experiments with increased sensitivity. While the gauge symmetry is necessary to induce the new matter effect, the observables only depend on the size of the scalar VEVs and not on the gauge coupling. The neutrino NSI thus probe the scale of the symmetry breaking, which can be even above a few TeV and still lead to potentially observable effects.

As already mentioned in the Introduction, our model has an important ambiguity: which leptons should carry the new gauge quantum numbers. While for quarks the choice is clear — the top and bottom have very small mixing with the quarks from the other generations, which we are trying to explain — in the case of leptons there is no natural choice. We have so far considered the tau lepton and the corresponding neutrino, but only for definitiveness. From the point of view of anomaly cancelation, which was our guiding principle in selecting the flavor symmetry, any lepton flavor could have been selected to be charged under this new symmetry. This means that it is possible to generate any flavor diagonal neutrino non-standard interaction (ϵ_{ee} or $\epsilon_{\mu\mu}$) in a similar way.

Some of the constraints and future search strategies are different in this case and require a reanalysis. In particular, one important consequence of assigning the new U(1) charges to the muon instead of tau would be the effects of *non-universality* in bottom meson decays to electrons and muon. To this end, let us mention that our model is relevant to the recently reported anomaly [94] in $b \to s l^+ l^-$ decays (specifically, the ratio $\mathrm{BR}(B^0 \to K^{*0}\mu^+\mu^-)/\mathrm{BR}(B^0 \to K^{*0} e^+ e^-)$). This analysis will be reported elsewhere.

Another class of observables involves processes such as the $D - \bar{D}$ mixing, atomic parity violation, and Møller scattering: for a heavy mediator they probe a combination of

JHEP12(2017)096

VEVs in the Higgs sector, related to the $X - Z$ mixing, while for a low mediator mass they are also sensitive to the gauge coupling g_X. Although the current constraint from Møller scattering is not competitive with other bounds, the future MOLLER experiment at Jefferson Lab will improve the bound, and may even take a leading role in constraining some region of the parameter space.

A unique role is played by the process $\Upsilon \to \tau^+\tau^-$, which operates entirely in the third generation and gives the most direct access to the coupling g_X. Future B-factory data may improve the universality bound on Υ decays and further constrain third family gauge symmetries.

Finally, LHC searches for X boson production may also play a role in constraining the model. Z decays to $\tau^+\tau^- X$ and $b\bar{b}X$, although less constraining at the present time, are also a direct probe of g_X. Thus, for X masses below the Z mass, dedicated searches taking into account the differences in kinematics between two and three body decays of the Z may be interesting venues for future exploration. We also identify resonant X boson production decaying to τ pairs in association with b-jets as a promising search for heavier masses. We thus foresee the LHC phenomenology of our model to be rich.

Another area of phenomenology that deserves a close look is establishing astrophysical signatures of this scenario. The relevant discussion is deferred to a separate paper, mainly to keep the scope of the present work finite. In brief, supernova and stellar cooling considerations do yield constraints on certain parts of the parameter space (low mass and small coupling).

A number of theoretical directions must also be pursued. Among them is the origin of the neutrino mass in this framework. Phenomenologically, we know that the lepton mixing matrix is qualitatively different from the CKM one, and in particular third generation is in no way singled out in it. This perhaps suggests that the origins of the neutrino masses and quark masses are different. Indeed, in our model phenomenological viability *requires* that neutrino masses be generated by certain operators suppressed by the scale of the new symmetry breaking. Importantly, this scale is expected to be at the TeV scale due to anomaly cancelation and therefore can be within reach of the LHC and future collider experiments and, we hope, will motivate future searches.

Acknowledgments

We thank KITP Santa Barbara for hospitality and support (National Science Foundation under Grant No. PHY11-25915) during the "Present and Future Neutrino Physics" workshop, where this work was started. PM thanks the Oklahoma State University and SLAC for kind hospitality during the completion of this manuscript. We thank Lance Dixon, Sasha Khanov, Aneesh Manohar, Carlos Peña, Michael Peskin, and Renata Zukanovich Funchal for useful discussions. This work is supported by the U.S. Department of Energy Grants No. de-sc0010108 (KSB), DE-AC02-76SF00515 (AF) and de-sc0013699 (IM), and by the EU grants H2020-MSCA-ITN-2015/674896-Elusives (PM) and H2020-MSCA-2015-690575-InvisiblesPlus (PM). Fermilab is operated by the Fermi Research Alliance, LLC under contract No. DE-AC02-07CH11359 with the United States Department of Energy.

JHEP12(2017)096

A Contributions to B_d and B_s widths

In the model proposed, α and β, defined in eq. (2.2), would contribute to $b \to Xd$ and $b \to Xs$ transitions. An alternative version of this model would have the $\mathrm{U}(1)_X$ charge of ϕ_1 and s changed to $-1/3$. In that case, which would interchange the structure of the up and down Yukawa sectors in eq. (2.1), the off-diagonal couplings of the down sector, which will be called α and β as well, would also contribute to b FCNCs. Here we estimate the constraints on the off-diagonal couplings of the down-type quarks (valid for both versions of the model). The $B_d - \bar{B}_d$ and $B_s - \bar{B}_s$ mixings constraints discussed in section 2 would apply, though they are not very stringent.

The process $B_d \to \pi X$ would contribute to the total B_d width by the following amount (assuming $M_X \ll m_{B_d}$)

$$\Gamma(B_d \to \pi X) = \frac{1}{144\pi} |F_+(M_X^2)|^2 g_X^2 a^2 \frac{m_{B_d}^3}{M_X^2}, \tag{A.1}$$

where m_{B_d} is the B_d mass, and $F_+(q^2)$ is a form factor which can be determined by use of chiral perturbation theory for heavy hadrons (see e.g. ref. [57]). Requiring this partial width to be below the total width of the B_d translates into the constraint

$$g_X < 2.9 \times 10^{-5} \left(\frac{M_X}{100\,\mathrm{MeV}}\right) \left(\frac{|V_{ub}|}{a}\right). \tag{A.2}$$

A similar process could be considered, with $B^+ \to \pi^+ X$ and X further decaying to $\mu^+\mu^-$, leading to $B^+ \to \pi^+\mu^+\mu^-$. This branching ratio is measured to be 1.79×10^{-8} [39] and would constrain (requiring the new contribution not to exceed the measurement)

$$g_X < \frac{3.8 \times 10^{-10}}{\sqrt{\mathrm{BR}(X \to \mu^+\mu^-)}} \left(\frac{M_X}{100\,\mathrm{MeV}}\right) \left(\frac{|V_{ub}|}{a}\right). \tag{A.3}$$

For instance, for $a = V_{ub}$, if $t_\beta = 20$ then the $\mu\mu$ branching ratio is 2.5×10^{-7}, and thus $g_X < 8.4 \times 10^{-7}(M_X/100\,\mathrm{MeV})$, which should be compared to best limit of the model in the text, arising from neutrino oscillations, $g_X < 4 \times 10^{-3}(M_X/100\,\mathrm{MeV})$. For the B_s, the total width bound is stronger than the B_d case by an order of magnitude, since the Xbs coupling would be proportional to V_{cb} which is ten times larger than V_{ub}. More precisely, $g_X < 2.8 \times 10^{-6}(M_X/100\,\mathrm{MeV})$.

References

[1] M.E. Peskin and D.V. Schroeder, *An Introduction to Quantum Field Theory*, Reading, U.S.A., Addison-Wesley (1995), pg. 842 [INSPIRE].

[2] D.J. Gross and R. Jackiw, *Effect of anomalies on quasirenormalizable theories*, *Phys. Rev.* **D 6** (1972) 477 [INSPIRE].

JHEP12(2017)096

[3] J.C. Pati and A. Salam, *Lepton Number as the Fourth Color*, *Phys. Rev.* **D 10** (1974) 275 [*Erratum ibid.* **D 11** (1975) 703] [INSPIRE].

[4] R.E. Marshak and R.N. Mohapatra, *Quark-Lepton Symmetry and B-L as the* U(1) *Generator of the Electroweak Symmetry Group*, *Phys. Lett.* **B 91** (1980) 222 [INSPIRE].

[5] F. Wilczek and A. Zee, *Conservation or Violation of B-L in Proton Decay*, *Phys. Lett.* **B 88** (1979) 311 [INSPIRE].

[6] R.N. Mohapatra and R.E. Marshak, *Local B-L Symmetry of Electroweak Interactions, Majorana Neutrinos and Neutron Oscillations*, *Phys. Rev. Lett.* **44** (1980) 1316 [*Erratum ibid.* **44** (1980) 1643] [INSPIRE].

[7] A.E. Nelson and J. Walsh, *Short Baseline Neutrino Oscillations and a New Light Gauge Boson*, *Phys. Rev.* **D 77** (2008) 033001 [arXiv:0711.1363] [INSPIRE].

[8] R. Harnik, J. Kopp and P.A.N. Machado, *Exploring nu Signals in Dark Matter Detectors*, *JCAP* **07** (2012) 026 [arXiv:1202.6073] [INSPIRE].

[9] B. Holdom, *Two* U(1)*'s and Epsilon Charge Shifts*, *Phys. Lett.* **B 166** (1986) 196 [INSPIRE].

[10] F. Wilczek and A. Zee, *Horizontal Interaction and Weak Mixing Angles*, *Phys. Rev. Lett.* **42** (1979) 421 [INSPIRE].

[11] T. Appelquist and R. Shrock, *Neutrino masses in theories with dynamical electroweak symmetry breaking*, *Phys. Lett.* **B 548** (2002) 204 [hep-ph/0204141] [INSPIRE].

[12] T. Appelquist and R. Shrock, *Dynamical symmetry breaking of extended gauge symmetries*, *Phys. Rev. Lett.* **90** (2003) 201801 [hep-ph/0301108] [INSPIRE].

[13] X.-G. He, G.C. Joshi, H. Lew and R.R. Volkas, *Simplest Z′ model*, *Phys. Rev.* **D 44** (1991) 2118 [INSPIRE].

[14] S. Baek, N.G. Deshpande, X.G. He and P. Ko, *Muon anomalous g-2 and gauged* $L_\mu - L_\tau$ *models*, *Phys. Rev.* **D 64** (2001) 055006 [hep-ph/0104141] [INSPIRE].

[15] E. Ma, D.P. Roy and S. Roy, *Gauged* $L_\mu - L_\tau$ *with large muon anomalous magnetic moment and the bimaximal mixing of neutrinos*, *Phys. Lett.* **B 525** (2002) 101 [hep-ph/0110146] [INSPIRE].

[16] E. Salvioni, A. Strumia, G. Villadoro and F. Zwirner, *Non-universal minimal Z' models: present bounds and early LHC reach*, *JHEP* **03** (2010) 010 [arXiv:0911.1450] [INSPIRE].

[17] J. Heeck and W. Rodejohann, *Gauged* $L_\mu - L_\tau$ *Symmetry at the Electroweak Scale*, *Phys. Rev.* **D 84** (2011) 075007 [arXiv:1107.5238] [INSPIRE].

[18] K. Harigaya, T. Igari, M.M. Nojiri, M. Takeuchi and K. Tobe, *Muon g-2 and LHC phenomenology in the* $L_\mu - L_\tau$ *gauge symmetric model*, *JHEP* **03** (2014) 105 [arXiv:1311.0870] [INSPIRE].

[19] C.D. Carone, *Flavor-Nonuniversal Dark Gauge Bosons and the Muon g-2*, *Phys. Lett.* **B 721** (2013) 118 [arXiv:1301.2027] [INSPIRE].

[20] W. Altmannshofer, S. Gori, M. Pospelov and I. Yavin, *Quark flavor transitions in* $L_\mu - L_\tau$ *models*, *Phys. Rev.* **D 89** (2014) 095033 [arXiv:1403.1269] [INSPIRE].

[21] Y. Farzan, *A model for large non-standard interactions of neutrinos leading to the LMA-Dark solution*, *Phys. Lett.* **B 748** (2015) 311 [arXiv:1505.06906] [INSPIRE].

JHEP12(2017)096

[22] Y. Farzan and I.M. Shoemaker, *Lepton Flavor Violating Non-Standard Interactions via Light Mediators*, *JHEP* **07** (2016) 033 [arXiv:1512.09147] [INSPIRE].

[23] G. D'Ambrosio, G.F. Giudice, G. Isidori and A. Strumia, *Minimal flavor violation: An Effective field theory approach*, *Nucl. Phys.* **B 645** (2002) 155 [hep-ph/0207036] [INSPIRE].

[24] L. Wolfenstein, *Neutrino Oscillations in Matter*, *Phys. Rev.* **D 17** (1978) 2369 [INSPIRE].

[25] J.W.F. Valle, *Resonant Oscillations of Massless Neutrinos in Matter*, *Phys. Lett.* **B 199** (1987) 432 [INSPIRE].

[26] E. Roulet, *MSW effect with flavor changing neutrino interactions*, *Phys. Rev.* **D 44** (1991) R935 [INSPIRE].

[27] M.M. Guzzo, A. Masiero and S.T. Petcov, *On the MSW effect with massless neutrinos and no mixing in the vacuum*, *Phys. Lett.* **B 260** (1991) 154 [INSPIRE].

[28] M.C. Gonzalez-Garcia, Y. Grossman, A. Gusso and Y. Nir, *New CP-violation in neutrino oscillations*, *Phys. Rev.* **D 64** (2001) 096006 [hep-ph/0105159] [INSPIRE].

[29] N. Fornengo, M. Maltoni, R. Tomas and J.W.F. Valle, *Probing neutrino nonstandard interactions with atmospheric neutrino data*, *Phys. Rev.* **D 65** (2002) 013010 [hep-ph/0108043] [INSPIRE].

[30] S. Davidson, C. Pena-Garay, N. Rius and A. Santamaria, *Present and future bounds on nonstandard neutrino interactions*, *JHEP* **03** (2003) 011 [hep-ph/0302093] [INSPIRE].

[31] A. Friedland, C. Lunardini and C. Pena-Garay, *Solar neutrinos as probes of neutrino matter interactions*, *Phys. Lett.* **B 594** (2004) 347 [hep-ph/0402266] [INSPIRE].

[32] A. Friedland and C. Lunardini, *A test of tau neutrino interactions with atmospheric neutrinos and K2K*, *Phys. Rev.* **D 72** (2005) 053009 [hep-ph/0506143] [INSPIRE].

[33] S. Antusch, J.P. Baumann and E. Fernandez-Martinez, *Non-Standard Neutrino Interactions with Matter from Physics Beyond the Standard Model*, *Nucl. Phys.* **B 810** (2009) 369 [arXiv:0807.1003] [INSPIRE].

[34] M.B. Gavela, D. Hernandez, T. Ota and W. Winter, *Large gauge invariant non-standard neutrino interactions*, *Phys. Rev.* **D 79** (2009) 013007 [arXiv:0809.3451] [INSPIRE].

[35] M.C. Gonzalez-Garcia, M. Maltoni and J. Salvado, *Testing matter effects in propagation of atmospheric and long-baseline neutrinos*, *JHEP* **05** (2011) 075 [arXiv:1103.4365] [INSPIRE].

[36] A. Friedland, M.L. Graesser, I.M. Shoemaker and L. Vecchi, *Probing Nonstandard Standard Model Backgrounds with LHC Monojets*, *Phys. Lett.* **B 714** (2012) 267 [arXiv:1111.5331] [INSPIRE].

[37] A. Friedland and I.M. Shoemaker, *Searching for Novel Neutrino Interactions at NOvA and Beyond in Light of Large θ_{13}*, arXiv:1207.6642 [INSPIRE].

[38] M.C. Gonzalez-Garcia, M. Maltoni and T. Schwetz, *Global Analyses of Neutrino Oscillation Experiments*, *Nucl. Phys.* **B 908** (2016) 199 [arXiv:1512.06856] [INSPIRE].

[39] Particle Data Group collaboration, K.A. Olive et al., *Review of Particle Physics*, *Chin. Phys.* **C 38** (2014) 090001 [INSPIRE].

[40] F. Vissani, *Do experiments suggest a hierarchy problem?*, *Phys. Rev.* **D 57** (1998) 7027 [hep-ph/9709409] [INSPIRE].

JHEP12(2017)096

[41] M. Baumgart, C. Cheung, J.T. Ruderman, L.-T. Wang and I. Yavin, *Non-Abelian Dark Sectors and Their Collider Signatures*, *JHEP* **04** (2009) 014 [arXiv:0901.0283] [INSPIRE].

[42] G.C. Branco, P.M. Ferreira, L. Lavoura, M.N. Rebelo, M. Sher and J.P. Silva, *Theory and phenomenology of two-Higgs-doublet models*, *Phys. Rept.* **516** (2012) 1 [arXiv:1106.0034] [INSPIRE].

[43] ATLAS, CMS collaborations, *Measurements of the Higgs boson production and decay rates and constraints on its couplings from a combined ATLAS and CMS analysis of the LHC pp collision data at $\sqrt{s} = 7$ and 8 TeV*, *JHEP* **08** (2016) 045 [arXiv:1606.02266] [INSPIRE].

[44] CMS collaboration, *Search for a heavy Higgs boson in the H to ZZ to 2l2nu channel in pp collisions at $\sqrt{s} = 7$ and 8 TeV*, CMS-PAS-HIG-13-014.

[45] ATLAS collaboration, *Search for an additional, heavy Higgs boson in the $H \to ZZ$ decay channel at $\sqrt{s} = 8$ TeV in pp collision data with the ATLAS detector*, *Eur. Phys. J.* **C 76** (2016) 45 [arXiv:1507.05930] [INSPIRE].

[46] T. Hermann, M. Misiak and M. Steinhauser, *$\bar{B} \to X_s\gamma$ in the Two Higgs Doublet Model up to Next-to-Next-to-Leading Order in QCD*, *JHEP* **11** (2012) 036 [arXiv:1208.2788] [INSPIRE].

[47] ATLAS collaboration, *Search for charged Higgs bosons in the $H^\pm \to tb$ decay channel in pp collisions at $\sqrt{s} = 8$ TeV using the ATLAS detector*, *JHEP* **03** (2016) 127 [arXiv:1512.03704] [INSPIRE].

[48] R. Essig et al., *Working Group Report: New Light Weakly Coupled Particles*, arXiv:1311.0029 [INSPIRE].

[49] M.R. Whalley, *A Compilation of data on hadronic total cross-sections in e^+e^- interactions*, *J. Phys.* **G 29** (2003) A1 [INSPIRE].

[50] http://hepdata.cedar.ac.uk/review/rsig/.

[51] BABAR collaboration, P. del Amo Sanchez et al., *Test of lepton universality in $\Upsilon(1S)$ decays at BaBar*, *Phys. Rev. Lett.* **104** (2010) 191801 [arXiv:1002.4358] [INSPIRE].

[52] A.V. Manohar and P. Ruiz-Femenia, *The Orthopositronium decay spectrum using NRQED*, *Phys. Rev.* **D 69** (2004) 053003 [hep-ph/0311002] [INSPIRE].

[53] K. Blum, Y. Grossman, Y. Nir and G. Perez, *Combining K^0-$\bar{K}^0$ mixing and D^0-$\bar{D}^0$ mixing to constrain the flavor structure of new physics*, *Phys. Rev. Lett.* **102** (2009) 211802 [arXiv:0903.2118] [INSPIRE].

[54] K.S. Babu and Y. Meng, *Flavor Violation in Supersymmetric Q(6) Model*, *Phys. Rev.* **D 80** (2009) 075003 [arXiv:0907.4231] [INSPIRE].

[55] K.S. Babu and S. Nandi, *Natural fermion mass hierarchy and new signals for the Higgs boson*, *Phys. Rev.* **D 62** (2000) 033002 [hep-ph/9907213] [INSPIRE].

[56] E. Golowich, J. Hewett, S. Pakvasa and A.A. Petrov, *Relating D^0-$\bar{D}^0$ Mixing and $D^0 \to \ell^+\ell^-$ with New Physics*, *Phys. Rev.* **D 79** (2009) 114030 [arXiv:0903.2830] [INSPIRE].

[57] G. Burdman and I. Shipsey, *D^0-$\bar{D}^0$ mixing and rare charm decays*, *Ann. Rev. Nucl. Part. Sci.* **53** (2003) 431 [hep-ph/0310076] [INSPIRE].

[58] K.S. Babu, X.G. He, X. Li and S. Pakvasa, *Fourth Generation Signatures in D^0-$\bar{D}^0$ Mixing and Rare D Decays*, *Phys. Lett.* **B 205** (1988) 540 [INSPIRE].

[59] W.J. Marciano and Z. Parsa, *Rare kaon decays with "missing energy"*, *Phys. Rev.* **D 53** (1996) R1.

JHEP12(2017)096

[60] E949 collaboration, V.V. Anisimovsky et al., *Improved measurement of the $K^+ \to \pi^+ \nu\bar{\nu}$ branching ratio*, *Phys. Rev. Lett.* **93** (2004) 031801 [hep-ex/0403036] [INSPIRE].

[61] P. Ball and R. Zwicky, *New results on $B \to \pi, K, \eta$ decay formfactors from light-cone sum rules*, *Phys. Rev.* **D 71** (2005) 014015 [hep-ph/0406232] [INSPIRE].

[62] E949 collaboration, A.V. Artamonov et al., *New measurement of the $K^+ \to \pi^+ \nu\bar{\nu}$ branching ratio*, *Phys. Rev. Lett.* **101** (2008) 191802 [arXiv:0808.2459] [INSPIRE].

[63] T. Inami and C.S. Lim, *Effects of Superheavy Quarks and Leptons in Low-Energy Weak Processes $K_L \to \mu\bar{\mu}$, $K^+ \to \pi^+ \nu\bar{\nu}$ and $K^0 \to \bar{K}^0$*, *Prog. Theor. Phys.* **65** (1981) 297 [*Erratum ibid.* **65** (1981) 1772] [INSPIRE].

[64] L.J. Hall and M.B. Wise, *Flavor changing Higgs-boson couplings*, *Nucl. Phys.* **B 187** (1981) 397 [INSPIRE].

[65] J.M. Frere, J.A.M. Vermaseren and M.B. Gavela, *The Elusive Axion*, *Phys. Lett.* **B 103** (1981) 129 [INSPIRE].

[66] M. Freytsis, Z. Ligeti and J. Thaler, *Constraining the Axion Portal with $B \to K l^+ l^-$*, *Phys. Rev.* **D 81** (2010) 034001 [arXiv:0911.5355] [INSPIRE].

[67] H. Davoudiasl, H.-S. Lee and W.J. Marciano, *'Dark' Z implications for Parity Violation, Rare Meson Decays and Higgs Physics*, *Phys. Rev.* **D 85** (2012) 115019 [arXiv:1203.2947] [INSPIRE].

[68] M.C. Gonzalez-Garcia and M. Maltoni, *Determination of matter potential from global analysis of neutrino oscillation data*, *JHEP* **09** (2013) 152 [arXiv:1307.3092] [INSPIRE].

[69] S.G. Porsev, K. Beloy and A. Derevianko, *Precision determination of weak charge of ^{133}Cs from atomic parity violation*, *Phys. Rev.* **D 82** (2010) 036008 [arXiv:1006.4193] [INSPIRE].

[70] ATLAS collaboration, *Search for invisible decays of a Higgs boson using vector-boson fusion in pp collisions at $\sqrt{s} = 8$ TeV with the ATLAS detector*, *JHEP* **01** (2016) 172 [arXiv:1508.07869] [INSPIRE].

[71] SLAC E158 collaboration, P.L. Anthony et al., *Observation of parity nonconservation in Moller scattering*, *Phys. Rev. Lett.* **92** (2004) 181602 [hep-ex/0312035] [INSPIRE].

[72] W.J. Marciano and D. Wyler, *W production via Z decay*, *Z. Phys.* **C 3** (1979) 181 [INSPIRE].

[73] CMS collaboration, *Search for pair production of third-generation leptoquarks and top squarks in pp collisions at $\sqrt{s} = 7$ TeV*, *Phys. Rev. Lett.* **110** (2013) 081801 [arXiv:1210.5629] [INSPIRE].

[74] ATLAS collaboration, *Search for third generation scalar leptoquarks in pp collisions at $\sqrt{s} = 7$ TeV with the ATLAS detector*, *JHEP* **06** (2013) 033 [arXiv:1303.0526] [INSPIRE].

[75] Y. Nir and D.J. Silverman, *Z Mediated Flavor Changing Neutral Currents and Their Implications for CP Asymmetries in B^0 Decays*, *Phys. Rev.* **D 42** (1990) 1477 [INSPIRE].

[76] A.J. Buras, M. Jamin and P.H. Weisz, *Leading and Next-to-leading QCD Corrections to ϵ Parameter and $B^0 - \bar{B}^0$ Mixing in the Presence of a Heavy Top Quark*, *Nucl. Phys.* **B 347** (1990) 491 [INSPIRE].

[77] A. Lenz, *Theoretical update of B-Mixing and Lifetimes*, arXiv:1205.1444 [INSPIRE].

[78] J.D. Bjorken, R. Essig, P. Schuster and N. Toro, *New Fixed-Target Experiments to Search for Dark Gauge Forces*, *Phys. Rev.* **D 80** (2009) 075018 [arXiv:0906.0580] [INSPIRE].

JHEP12(2017)096

[79] A.I. Studenikin, *Charged lepton G-2 and constraints on new physics*, hep-ph/9808219 [INSPIRE].

[80] F. Jegerlehner and A. Nyffeler, *The Muon g-2*, *Phys. Rept.* **477** (2009) 1 [arXiv:0902.3360] [INSPIRE].

[81] BESIII collaboration, M. Ablikim et al., *Precision measurement of the mass of the τ lepton*, *Phys. Rev.* **D 90** (2014) 012001 [arXiv:1405.1076] [INSPIRE].

[82] G. Bellini et al., *Precision measurement of the ^{7}Be solar neutrino interaction rate in Borexino*, *Phys. Rev. Lett.* **107** (2011) 141302 [arXiv:1104.1816] [INSPIRE].

[83] A.G. Beda et al., *GEMMA experiment: Three years of the search for the neutrino magnetic moment*, *Phys. Part. Nucl. Lett.* **7** (2010) 406 [arXiv:0906.1926] [INSPIRE].

[84] CHARM-II collaboration, P. Vilain et al., *Precision measurement of electroweak parameters from the scattering of muon-neutrinos on electrons*, *Phys. Lett.* **B 335** (1994) 246 [INSPIRE].

[85] TEXONO collaboration, M. Deniz et al., *Measurement of $\bar{\nu}_e$-Electron Scattering Cross-Section with a CsI(Tl) Scintillating Crystal Array at the Kuo-Sheng Nuclear Power Reactor*, *Phys. Rev.* **D 81** (2010) 072001 [arXiv:0911.1597] [INSPIRE].

[86] MiniBooNE collaboration, A.A. Aguilar-Arevalo et al., *A Search for electron neutrino appearance at the $\Delta m^2 \sim 1\, eV^2$ scale*, *Phys. Rev. Lett.* **98** (2007) 231801 [arXiv:0704.1500] [INSPIRE].

[87] MiniBooNE collaboration, A.A. Aguilar-Arevalo et al., *A Combined $\nu_\mu \to \nu_e$ and $\bar{\nu}_\mu \to \bar{\nu}_e$ Oscillation Analysis of the MiniBooNE Excesses*, arXiv:1207.4809 [INSPIRE].

[88] LSND collaboration, L.B. Auerbach et al., *Measurement of electron-neutrino-electron elastic scattering*, *Phys. Rev.* **D 63** (2001) 112001 [hep-ex/0101039] [INSPIRE].

[89] NuTeV collaboration, G.P. Zeller et al., *A precise determination of electroweak parameters in neutrino nucleon scattering*, *Phys. Rev. Lett.* **88** (2002) 091802 [*Erratum ibid.* **90** (2003) 239902] [hep-ex/0110059] [INSPIRE].

[90] L3 collaboration, M. Acciarri et al., *Search for manifestations of new physics in fermion pair production at LEP*, *Phys. Lett.* **B 489** (2000) 81 [hep-ex/0005028] [INSPIRE].

[91] B. Batell, M. Pospelov and A. Ritz, *Exploring Portals to a Hidden Sector Through Fixed Targets*, *Phys. Rev.* **D 80** (2009) 095024 [arXiv:0906.5614] [INSPIRE].

[92] TEXONO collaboration, H.T. Wong et al., *A Search of Neutrino Magnetic Moments with a High-Purity Germanium Detector at the Kuo-Sheng Nuclear Power Station*, *Phys. Rev.* **D 75** (2007) 012001 [hep-ex/0605006] [INSPIRE].

[93] J.-W. Chen et al., *Constraints on millicharged neutrinos via analysis of data from atomic ionizations with germanium detectors at sub-keV sensitivities*, *Phys. Rev.* **D 90** (2014) 011301 [arXiv:1405.7168] [INSPIRE].

[94] S. Bifani, *Search for New Physics with $b \to sll$ decays at LHCb*, CERN seminar, 18 April 2017.

JHEP12(2017)096